Geoderma 434 (2023) 116477

Contents lists available at ScienceDirect

Geoderma

journal homepage: www.elsevier.com/locate/geoderma

# Active plant biomass inputs influence pore system functioning in no-till soils

Cristhian Hernandez Gamboa [a,*], Getulio Coutinho Figueiredo [b], Fabiane Machado Vezzani [c], Fabíola Carenhatto Ferreira [d], Cimélio Bayer [b]

[a] Graduate Program in Soil Science, Federal University of Rio Grande do Sul (UFRGS), Av. Bento Gonçalves, 7712 - Agronomia, 91540-000 Porto Alegre, RS, Brazil
[b] Department of Soil Science, Federal University of Rio Grande do Sul (UFRGS), Av. Bento Gonçalves, 7712 - Agronomia, 91540-000 Porto Alegre, RS, Brazil
[c] Department of Soil Science and Agriculture Engineering, Federal University of Paraná (UFPR), Rua dos Funcionários, 1540 - Juvevê Curitiba, 80035-050 PR, Brazil
[d] Undergraduate Program in Agronomy, Federal University of Rio Grande do Sul (UFRGS), Av. Bento Gonçalves, 7712 - Agronomia, 91540-000 Porto Alegre, RS, Brazil

ARTICLE INFO

Handling Editor: Alberto Agnelli

*Keywords:*
Pore network continuity
Air fluxes
Water fluxes
Soil self-organization
Cropping systems
No-till

ABSTRACT

Available knowledge about the exact impact of plant growth on the properties and functioning of no-till soils is somewhat limited, especially in tropical and subtropical regions. The starting hypothesis for this work was that long-term active plant biomass Input-APBI (aboveground plant shoot biomass) would improve pore system functioning in surface and subsurface soil layers by playing different, complementary roles in a previously degraded subtropical Acrisol. The hypothesis was checked by examining the results of a 34-yr field experiment involving five different cropping systems, namely: bare soil (BS), perennial pasture (PAST), oat/maize (O/M), oat + vetch/maize (O + V/M) and oat + vetch/ maize + cowpea (O + V/M + C). The soil was supplied with APBIs varying from 0.13 to 1.48 kg dry matter $ha^{-1}$ $yr^{-1}$. The APBIs for each cropping system were very low (BS), low (O/M), medium (O + V/M), high (O + V/M + C), and very high (PAST). The surface (0–5 cm) and subsurface (5–15 cm) soil layer were analyzed for static and dynamic properties of the pore system including bulk density; total, macro, and microporosity; the ability of the system to conduct air and water; continuity in soil pores; and plant-available water capacity. Micromorphological images of the soil revealed a complex pore network whose structure and functioning were both improved by the action of plants. In the surface soil layer, very high APBIs from pasture and high inputs from O + V/M + C increased total porosity by 11 and 14 %, respectively; pore continuity ($N_{cont}$) by 11 and 40 %, respectively; and microporosity by 31 and 23 %, respectively —all relative to bare soil. In the subsurface soil layer, pasture, and O + V/M + C decreased $N_{cont}$ by 44 and 40 %, respectively, but increased water permeability ($k_w$) by a factor of 6.5 and 7, respectively. In addition, very high APBIs increased continuity and permeability to air in macropores relative to BS. Organized large macropores in the subsurface soil layer efficiently conducted water and air from the soil surface and acted as bridges between the surface and subsurface soil layer. Overall, our findings suggest that APBIs helped develop a pore system with differential properties and complementary functions that influenced water infiltration and air fluxes in the surface soil layer, and water availability to crops in the subsurface soil layer, through long-term self-

*Abbreviations:* APBIs, active plant biomass inputs; BS, bare soil; O/M, **oat**/maize; O+V/M, **oat**+**vetch**/maize; O+V/M+C, **oat**+**vetch**/maize+**cowpea**; PAST, perennial pasture; BD, bulk density; TP, total porosity; Ɛ, air filled porosity; $MAC_{(300)}$, aeration porosity (pores with an equivalent diameter > 300 μm); $MAC_{(50)}$, macroporosity (pores with an equivalent diameter >50 μm); MIC, microporosity; μ, gravimetric water content; θ, volumetric water content; $k_{a(300)}$, intrinsic permeability to air in pores with an equivalent diameter > 300 μm; $k_{a(50)}$, intrinsic permeability to air in pores with an equivalent diameter > 50 μm; $k_{a(0.6)}$, intrinsic permeability to air in pores with an equivalent diameter > 0.6 μm; $k_{sat}$, saturated hydraulic conductivity; $k'_{sat}$, saturated hydraulic conductivity corrected to 20 °C; $k_w$, intrinsic permeability to water; $k_{1(300)}$, pore organization index ($k_{a(300)}/\varepsilon$) with an equivalent diameter > 300 μm; $k_{1(50)}$, pore organization index ($k_{a(50)}/\varepsilon$) with an equivalent diameter > 50 μm; $k_{1(0.6)}$, pore organization index ($k_{a(0.6)}/\varepsilon$) with an equivalent diameter > 0.6 μm; $k_{2(300)}$, pore organization index ($k_{a(300)}/\varepsilon^2$) with an equivalent diameter > 300 μm; $k_{2(50)}$, pore organization index ($k_{a(50)}/\varepsilon^2$) with an equivalent diameter > 50 μm; $k_{2(0.6)}$, pore organization index ($k_{a(0.6)}/\varepsilon^2$) with an equivalent diameter > 0.6 μm; $N_{cont}$, overall pore continuity index; $Ɛ_b$, blocked porosity to aeration; PAWC, plant-available water capacity; RD, root density; SOC, soil organic carbon; SWRC, soil water retention curve.

* Corresponding author.
*E-mail addresses:* cuentadoctoradocris@gmail.com (C. Hernandez Gamboa), getulio.figueiredo@ufrgs.br (G. Coutinho Figueiredo), vezzani@ufpr.br (F. Machado Vezzani), fabi_carenhatto@hotmail.com (F. Carenhatto Ferreira), cimelio.bayer@ufrgs.br (C. Bayer).

https://doi.org/10.1016/j.geoderma.2023.116477
Received 6 June 2022; Received in revised form 12 April 2023; Accepted 16 April 2023
Available online 27 April 2023

organization in the system. Future research with a view to understanding the influence of species richness and roots on physical quality in no-till soils is recommended.

## 1. Introduction

Plants are known to strongly influence the properties and functioning of soil (Goebes et al., 2019; Zhang and Peng, 2021). The influence has evolved since soil formed about 460–470 million years by effect of microbes (Brundrett, 2002) and primitive plants colonizing and transforming rocks through rhizoids, rhizomes, and other structures (Pawlik et al., 2016). The presence of vegetation with a wide variety of plant species is essential to maintain a permanent cover over soil in order to protect it, preserve ecosystem functions, and sustain life (Labrière et al., 2015). Thus, complex, diversified cropping systems with a high plant richness (Altieri, 1999; Gamboa et al., 2020) have been shown to facilitate ecological restoration (Barral et al., 2015), and increase self-organization and quality in agricultural soils (Anghinoni and Vezzani, 2021). The self-organization entails soil changes promoted by interactions of plants with biota and minerals, and its intensity depends on energy and C fluxes generated by developing plants (Anghinoni and Vezzani, 2021; Vezzani and Mielniczuk, 2011a). Self-organization processes are evidenced in the formation of stable aggregates (Vezzani and Mielniczuk, 2011b), the increase of C and N in microbial biomass (Chen et al., 2020), and the accumulation of soil organic matter (Veloso et al., 2019).

The interaction of plant biomass with soil biota (Brundrett, 2002) influences the physical and chemical properties of soil, and also the formation of pore networks. The primary action of roots is mechanical and results in soil deformation around growing roots, relocate of material and formation of a complex pore network (Cui et al., 2019; Keyes et al., 2016; Tisdall and Oades, 1982) that facilitates access to resources such as water, air, and nutrients (Pawlik et al., 2016; Pierret et al., 2007).

As regards soil formation, plants promote the differentiation of surface and subsurface soil horizons or layers (Brimhall et al., 1991; Goebes et al., 2019; Pawlik et al., 2016) with distinct yet integrated pore systems that play complementary roles (Minasny et al., 2016). The soil pore system affects dynamic processes including water infiltration and storage, and gas fluxes (Reynolds et al., 2009), which are essential for biota to function properly and also for soil preservation, root growth, and plant production (Pagliai and Vignozzi, 2002). Rhizodeposition of organic compounds from roots also impacts soil during their life cycle (Jones et al., 2009). The effect of the root system continues well after plants have died or been harvested as a result of soil biota decomposing roots, and biopores remaining in soil influencing nutrient, air, and water movement across the soil profile (Lavelle et al., 2006). In addition to the presence of plants, the minimal mechanical disturbance in no-till soils preserves the connected pore network, thus helping increase belowground water and nutrient use efficiency (FAO, 2020; Oberč and Arroyo Schnell, 2020).

Aboveground plant shoot biomass per unit surface (Westlake, 1963), which is referred to as "Active Plant Biomass Inputs" (APBIs) and expressed in kg dry matter (DM) per $m^2$ here, can be used to indicate the magnitude of energy and C flows in soil. Flows come mainly from plant rhizodeposition and deposition of residues onto the soil surface. High energy and C flows have a favorable effect on the interactions of minerals, organic matter and microbes that influence physical, chemical and biological properties of soil; also, they promote a complex process of soil self-organization (Anghinoni and Vezzani, 2021). The effect can be ascribed to changes in physical-hydraulic attributes of soil, as well as to the functioning of its pore system. Analyzing the self-organization effect of plants requires examining attributes that influence dynamic processes in soil (Poulsen, 2013). For example, air permeability (Ball and Schjønning, 2002) is a measure of the ability of soil to conduct gases (Dörner and Horn, 2006), when related to air-filled porosity it allows to assess the organization in terms of continuity (Groenevelt et al., 1984). Similarly, measurements of soil water fluxes including saturated hydraulic conductivity (Ellies Sch et al., 1997) and intrinsic water permeability (Reeve, 1953) can be directly related to the geometry of the pore system (Whelan et al., 1995) and its ability to conduct water.

The importance of plants for soil quality has traditionally been assessed mainly by examining physical degradation in soils under native vegetation following agricultural use (Alvarez et al., 2018; Kravchenko et al., 2011; Mudgal et al., 2010). However, recent studies have evidenced the influence of plants in a gradual, cumulative quality improvement in no-till soils remaining undisturbed for an extended period (Calonego and Rosolem, 2010; da Silva et al., 2021). Such studies have provided evidence for the positive impact of plants on the physical properties of no-till soils, especially in the form of a decreased bulk density (Bertollo et al., 2021; Sequinatto et al., 2014); an increased saturated hydraulic conductivity ($k_{sat}$) and water infiltration rate (Da-Silva et al., 2012; Singh et al., 2020); also increased water retention (Burgos Hernández et al., 2019; Lawal and Lawal, 2017); and improved larger pores (Farahani et al., 2022) and $k_{sat}$ in subsurface layers (Silva et al., 2008).

The primary aim of this work was to understand how plants, as a source of energy and C flows for soil, improve pore system functioning in the surface and subsurface layers of a no-till soil that had previously been degraded by inappropriate management for almost two decades. The starting hypothesis was that APBIs from no-till cropping systems would improve the pore system in the two layers and that the two systems would play different, complementary roles. Thus, we reasoned that the pore network in the surface soil layer acts mainly in the infiltration and conduction of water and air fluxes, whereas that in the subsurface layer influences water storage and availability to crops by preserving the ability of the soil to mobilize air and water, albeit to a lesser extent.

## 2. Material and methods

### 2.1. Site description

This work was based on a long-term (34 yr) field experiment established in 1983 on a sandy clay loam Acrisol at the Experimental Station of the Universidade Federal do Rio Grande do Sul, Eldorado do Sul, RS, in southern Brazil. Until 1969, the soil was covered by natural pasture typical of the Pampa biome (Brandão et al., 2007), with *Paspalum*, *Andropogon,* and *Desmodium* as the prevailing species. Then, the native vegetation was replaced with small grain crops and the soil intensively managed with plowing, harrowing, and removal of crop residues for about 14 years (until 1983). In that period, the soil was compacted (bulk density 1.68 Mg $m^{-3}$) and had a low macroporosity [4 % in the subsurface soil layer (10–30 cm); Pedó, 1986]. The initial organic matter content was 2 % (Bayer et al., 2000). Table 1 summarizes the properties of the soil and the regional climate.

### 2.2. Field experiment

Although the ongoing experiment involves ten cropping systems grown on no-till soil, only five were used here to assess the influence of APBIs on the pore system (Fig. 1). Thus, three of the treatments involved maize as summer crop plus one (**oat**/maize, O/M), two (**oat** + **vetch**/maize, O + V/M) or three cover crops (**oat** + **vetch**/maize + **cowpea**, O + V/M + C) for increased APBIs (Fig. 1). The other two treatments were bare soil (BS) and perennial pasture (PAST), which had very low and very high APBIs, respectively. The characteristics of the cropping

**Table 1**
Main soil and climate features at the experimental site in southern Brazil.

| Geographic coordinates | 30° 51′ S, 51° 38′ W |
|---|---|
| Altitude (m) | 96 |
| Köppen's climate class | Cfa |
| Mean annual precipitation (mm) | 1440 |
| Soil classification[a] | |
| FAO (WRB) | Acrisol |
| US taxonomy | Typic Paleudult |
| Grain size distribution 0–20 cm (clay, silt and sand, g kg$^{-1}$)[b] | 220, 240, 540 |
| Main minerals in clay fraction[c] | |
| Kaolinite (g kg$^{-1}$) [b] | 720 |
| Total iron oxides (g kg$^{-1}$) | 11.8 |
| Low-ordered iron oxides (g kg$^{-1}$) | 0.9 |
| Low-ordered/total iron oxide ratio | 0.1 |
| Goethite/(Goethite + Hematite) [d] | 0.1 |
| Soil Bulk Density (Mg m$^{-3}$)[e] at start of experiment (1983) | |
| 0–5 cm layer | 1.56 |
| 5–15 cm layer | 1.68 |

[a] IUSS FAO Working Group WRB (2015) and USDA-NRCS (2014) [b] Bayer et al. (2000) [c,d] Inda Junior et al. (2007) [e] Pedó (1986)

systems are illustrated in Fig. 1.

The specific crops used were oat (*Avena strigosa* Schreb), vetch (*Vicia sativa* L.), cowpea (*Vigna unguiculata* L. Walp), maize (*Zea mays* L.), and Pangola grass (*Digitaria decumbens* L.). A few plants of *Commelina benghalensis*, *Conyza* spp, *Eleusine indica,* and *Lolium multiflorum* were sporadically encountered in the BS treatment despite chemical and manual control of weeds. The field experiment followed a randomized complete block design with three replications, and plot size was 4 × 5 m (Fig. 2).

Winter cover crops (oat and oat + vetch consortium) were sown by direct drilling in April each year, using a distance of 0.17 m between rows and a seed density of 70–80 kg ha$^{-1}$. Maize was also sown by direct drilling from September to November (spring in the southern hemisphere), using a distance between rows of 0.90 m from 1983 to 2015, and 0.45 m afterwards. Cowpea was sown manually between maize rows approximately 20–30 days after maize, using a distance of 0.40 m between plants. Thus, with provision for machine traffic on the soil, it involved three operations each year, namely: (1) sowing of winter crops in autumn; (2) chemical desiccation of winter cover crops; and (3) sowing of maize. These operations were performed with a Valtra tractor Mod. 125i weighing 6.3 Mg, which, with provision for tire pressure, resulted in a final contact pressure of 144–149 kPa on soil.

The crops were supplied with water by sprinkler irrigation in the summer if needed. The fertilizer used consisted of 50 kg $K_2O$ ha$^{-1}$ and 50 kg $P_2O_5$ ha$^{-1}$, and was applied in the spring − summer season to the maize sowing rows. Fig. 1 shows further details of the cropping systems.

Aboveground plant shoot biomass per unit surface (kg DM m$^{-2}$ yr$^{-1}$) of cover crops, maize, pasture, and weeds, called here as active plant biomass input (APBI), was determined in the five treatments (BS, O/M, O + V/M, O + V/M + C, and PAST). The average input from each cropping system was obtained from the experiment dataset. A total of 11 measurements of plant biomass (shoots only) at the stage of maximal vegetative growth of the cover crops, maize (flowering) and Pangola grass, and also of weeds in the BS system, were made. These plant shoot measurements were made in 1985, 1986, 1988, 1989, 1993, 2008, 2010, 2011, and 2012. The average APBI for each cropping system was classified as very low (BS), low (O/M), medium (O + V/M), high (O + V/M + C), or very high (PAST). For this purpose, an input of 0.97 kg DM m$^{-2}$ yr$^{-1}$ was taken to be the minimum needed to maintain the organic C stock in the subtropical soil studied (Bayer et al., 2006), and the cropping system closest to that value was taken to represent a medium APBIs.

### 2.3. Soil sampling

Soil samples from the five cropping systems were collected in October 2017, which coincided with the end of the cycle of winter cover crops in O/M, O + V/M, and O + V/M + C. This evaluation at the end of the winter season was used to assess the cumulative effect of 34 years of no-till cropping rather than the short-term effect of the last cycle of winter cover crops. A total of 9 undisturbed soil samples were collected in volumetric rings 5.0 cm high and 5.66 cm in diameter (125.8 cm$^3$) for each treatment and soil layer. Therefore, 3 sub-samples per plot were collected from the surface layer (0–5 cm), and three others from subsurface layer (5–15 cm), between rows of the winter crops (Fig. 2). After

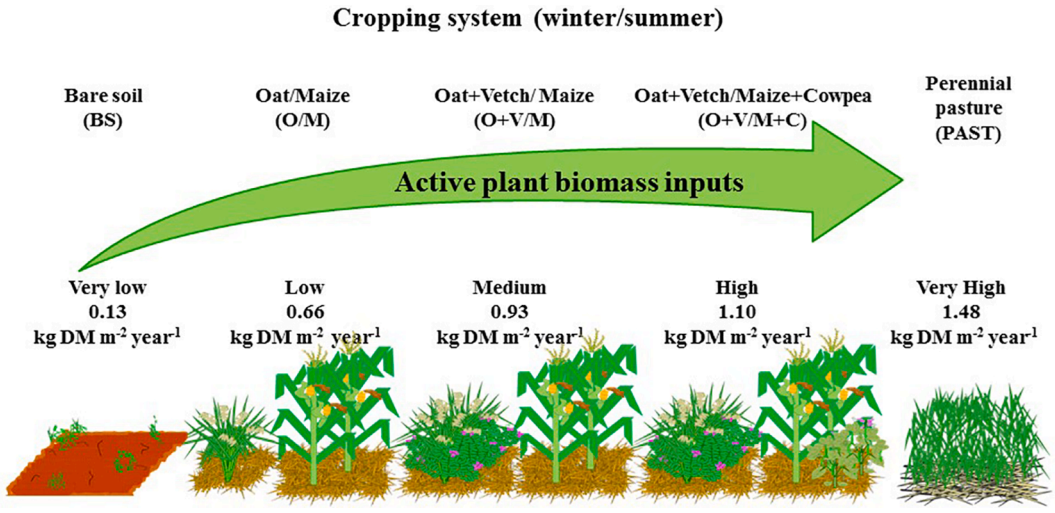


**Fig. 1.** Cropping systems (winter/summer species) and active plant biomass inputs (in Dry Matter). Characteristics of the crop and management systems: **(BS) Bare soil**, where spontaneous weeds were manually and mechanically managed or eventually desiccated with herbicide — except with maize under no-till in the 1988/89, 1993/94 and 1994/95 seasons. BS was not disturbed and there was no machine traffic at any time during the experimental period; **(O/M) Oat/Maize, (O + V/M) Oat + Vetch/Maize, (O + V/M + C) Oat + Vetch/Maize + Cowpea**, winter and summer crops seeded with direct drilling machine — cowpea was seeded by hand between maize rows. Winter and summer crops were terminated with a roller crimper. Weeds were controlled mechanically in the first 10 years and then by chemical desiccation with glyphosate-based herbicides; **(PAST) Perennial pasture**, under no machine traffic in the experimental period —excep maize was grown under no-till in the 1988/89, 1993/94, and 1994/95 summer seasons; pasture subjected to mowing by hand each spring/summer season. **ND** = not determined (weeds were mechanically managed or desiccated with herbicide). Active plant biomass input levels: very low, low, medium, high, and very high, defined in relation to the critical threshold needed to preserve the initial C stock in no-till soils: 0.97 kg m$^2$ (Bayer et al., 2006).

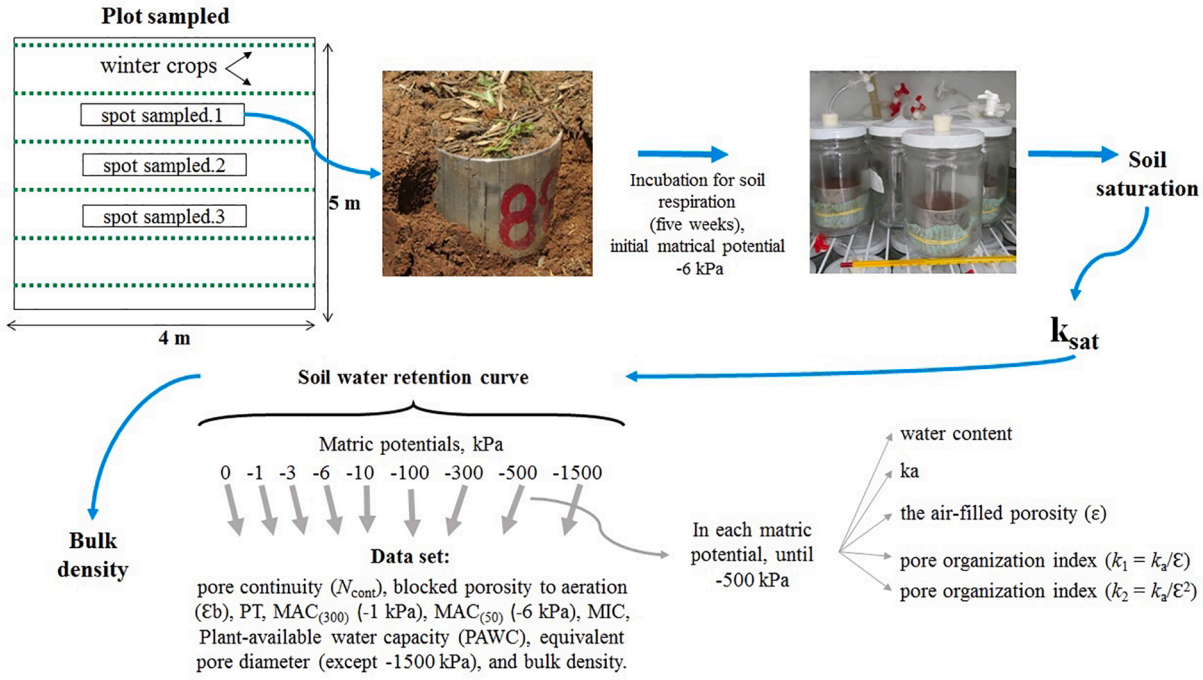


**Fig. 2.** Physico-hydric analysis. Phat of the undisturbed soil sample contained in the volumetric ring starting with the field sampling and the set of physical-hydraulic analyzes performed, for the quantification of the variables: BD (Mg $m^{-3}$), bulk density; TP ($m^3$ $m^{-3}$), soil total porosity; MAC$_{(300)}$ ($m^3$ $m^{-3}$), porosity of soil macropore domain; MAC$_{(50)}$ ($m^3$ $m^{-3}$), soil macroporosity; MIC ($m^3$ $m^{-3}$), soil microporosity; $k_{a(300)}$, $k_{a(50)}$, $k_{a(0.6)}$ ($\mu m^2$), soil intrinsic permeability to air in pores with equivalent diameter > 300, > 50, and > 0.6 μm, respectively; ksat (mm $h^{-1}$), saturated hydraulic conductivity; kw ($\mu m^2$), soil intrinsic permeability to water; $k_{1(300)}$, $k_{1(50)}$, $k_{1(0.6)}$ ($\mu m^2$ $m^{-3}$ $m^3$), pore organization indices with equivalent diameter > 300, > 50, and > 0.6 μm, respectively; $k_{2(300)}$, $k_{2(50)}$, $k_{2(0.6)}$ [$\mu m^2$ ($m^{-3}$ $m^3$)$^2$], pore organization indices with equivalent diameter > 300, > 50, and > 0.6 μm, respectively; $N_{cont}$, overall pore continuity; Ɛb (%), blocked porosity to aeration; PAWC (mm), plant-available water capacity;

careful removal of bulk soil around the cylinders, the collected samples were sealed with plastic film and transferred to the laboratory in closed containers for refrigeration at 4 °C until analysis.

### 2.4. Root parameters and soil organic carbon content

Root systems were examined by using the drill sampling method (Atkinson, 2000; Böhm, 1979). For this purpose, soil cores 133 and 267 $cm^3$ in volume were collected from the surface and subsurface soil layer, respectively, between rows of the winter crops. The samples were placed on sieves of 2.1 and 0.25 mm mesh, and jet water was gently applied to separate the soil from the roots. Then, the roots were dried at 40 °C to a constant mass and weighed. Root density was calculated as the ratio of soil dry mass to volume and expressed in kg $m^{-3}$ soil.

Additional soil samples were collected from the two soil layers for measurement of soil organic carbon (SOC). The samples were air-dried, ground, and passed through 2-mm mesh before grinding in an agate mortar. SOC was determined by dry combustion on a FlashEA 1112 elemental analyzer from Thermo Electron Corp. (Milan, Italy).

### 2.5. Physical-hydraulic analyses

Fig. 2 shows the path followed by the undisturbed soil samples contained in the volumetric rings from collection to analysis.

#### 2.5.1. Soil saturated hydraulic conductivity

This parameter ($k_{sat}$, m/s) was determined by using the falling head soil core method (Reynolds and Elrick, 2002) and calculated from the following equation:

$$k_{sat} = \left(\frac{a}{A_s}\right)\left(\frac{H}{t}\right) In\left(\frac{h_0}{h_1}\right) \quad (1)$$

where $a$ ($m^2$) is the cross-sectional diameter of the volumetric ring without soil, $A_s$ ($m^2$) that with soil, $H$ (m) the height of the volumetric ring with soil, $h_0$ (m) the initial hydraulic head, $h_1$ (m) the final hydraulic head, and $t$ (s) the time required for the hydraulic head, $h_0$, to equal $h_1$.

The $k_{sat}$ values thus obtained were adjusted to a water temperature of 20 °C by using eq. (2),

$$k'_{sat} = \frac{(k_{sat\ measured})\eta t}{\eta} \quad (2)$$

where $k'_{sat}$ is the soil saturated hydraulic conductivity as corrected to 20 °C; $k_{sat(measured)}$ the laboratory value of $k_{sat}$; $\eta t$ (N s $m^{-2}$) the water dynamic viscosity at the temperature $k_{sat}$ was measured and η that at 20 °C.

The intrinsic permeability of the soil to water, $k_w$ ($m^2$), was calculated from Darcy's equation (Reeve, 1953):

$$k_w = k'_{sat}\frac{\eta}{\rho g} \quad (3)$$

where $k'_{sat}$ is the saturated hydraulic conductivity, η the water dynamic viscosity, ρ the specific mass of water, and g the acceleration of gravity (m $s^{-2}$). Henceforth, $k'_{sat}$ will be called $k_{sat}$.

#### 2.5.2. Soil water retention curve

Once $k_{sat}$ was determined, the soil water retention curve (SWRC) was obtained by using a tension table at high matric potentials (0, –1, –3, –6, and –10 kPa), Richards' pressure plate apparatus at –33, –100 and –500 kPa with the volumetric ring containing the soil sample, and a Decagon Devices WP4-C psychrometer at the matric potential –1500 kPa with disturbed soil samples (Campbell, 2010). Once equilibrium at the different matric potentials was reached, each soil sample was weighed to calculate its volumetric water content (θ, $m^3$ $m^{-3}$; Libardi, 2016). SWRC

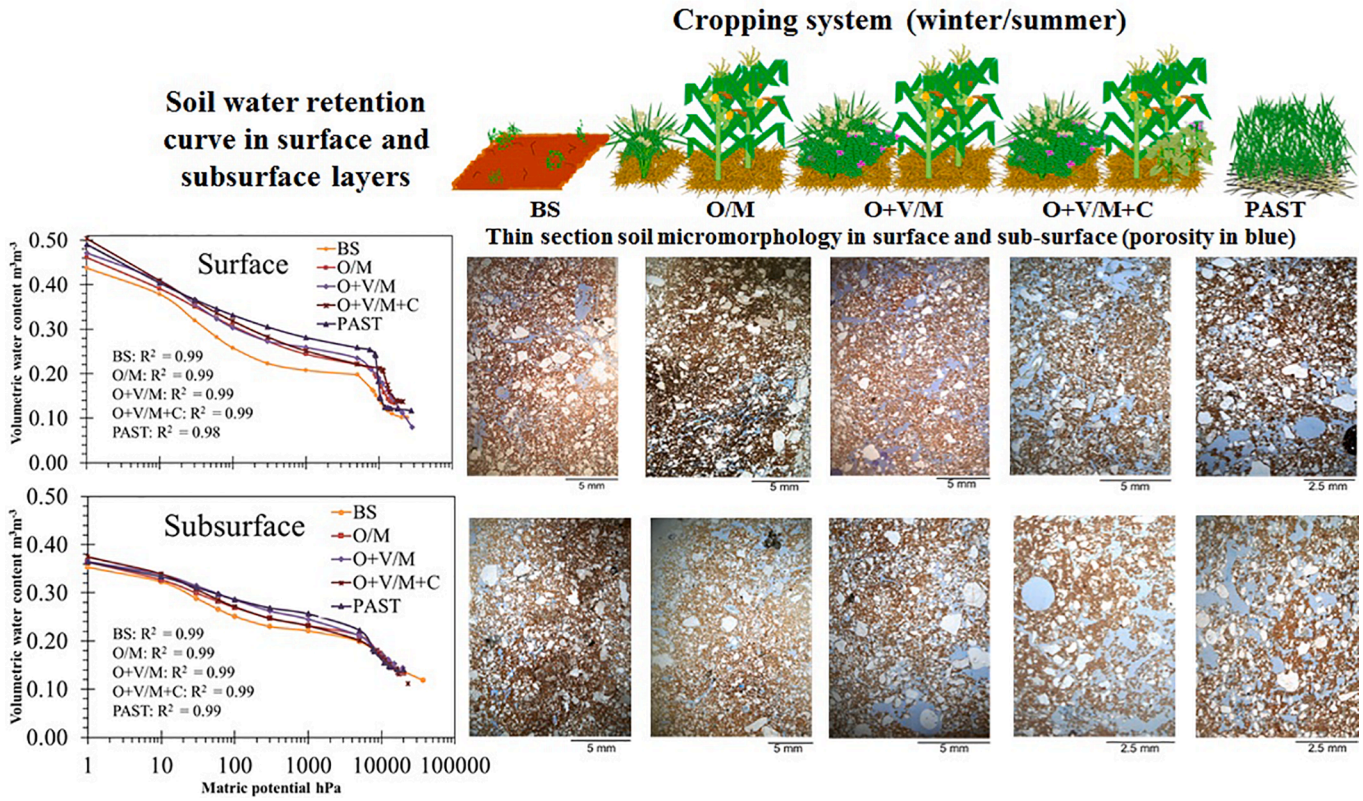


**Fig. 3.** Soil water retention curves and thin-section micromorphological images of the surface (0–5 cm) and subsurface layer (5–15 cm) of a no-till subtropical Acrisol with variable active plant biomass inputs (APBIs) for 34 years (BS, bare soil; PAST, perennial pasture) and improved APBIs + crop richness (O/M, oat/maize; O + V/M, oat + vetch/maize and O + V/M + C, oat + vetch/maize + cowpea). The blue color in the micromorphological sheets are pores filled by epoxy resin.

data were fitted by using the bimodal model of Seki (2007) with the aid of the software SWRC Fit (Seki, 2007):

$$Se = w1Q'\left(\frac{ln\left(\frac{h}{hm1}\right)}{\sigma 1}\right) + (1-w1)Q'\left(\frac{ln\left(\frac{h}{hm2}\right)}{\sigma 2}\right) \quad (4)$$

where $S_e$ is the effective saturation, given by $(\theta-\theta_r)/(\theta_s-\theta_r)$ [so, $\theta=\theta_r+(\theta_s-\theta_r)Se$]; $Q'(x)$ is the complementary normal distribution function [1–$\Phi(x)$, $\Phi(x)$ being a normalized form of the cumulative normal distribution function]; $w_1$ is the subcurve weighting factor; $\sigma_1$ and $\sigma_2$ are dimensionless fitting parameters generated by the model; $h$ is the water potential; and $hm_1$ and $hm_2$ are two fitting parameters.

### 2.5.3. Soil intrinsic permeability to air

All samples were weighed after reaching equilibrium at each matric potential (viz., –1, –3, –6, –10, –33, –100, and –500 kPa; Fig. 2). Air permeability was determined by using a constant head method (Prevedello and Armindo, 2015) involving application of an air flow (volumetric flow) at a gradually increasing constant rate to the samples in order to generate a potential difference. This way of determining $k_a$ holds under a laminar flow regime of gases through the sample (Reynolds number < 2000) (Ball and Schjønning, 2002; Silva et al., 2009). The intrinsic permeability to air, $k_a$ ($m^2$), was calculated from eq. (5), using the air flow rate through an area perpendicular to the fluid direction ($Q$) and the resulting potential difference ($dP/dz$), and assuming the air density to have a negligible influence:

$$k_a = \frac{Q\eta}{A_s}\left(\frac{dz}{dP}\right) \quad (5)$$

where $Q$ is the air flow rate ($m^3/s$), $A_s$ ($m^2$) the cross-sectional area of the volumetric ring containing the sample through which air flows, η (N s/$m^{-2}(-|-)$) the air dynamic viscosity, d$z$ (m) the distance in the direction air moves across the soil sample (i.e., the height of the volumetric ring), and d$P$ (Pa) the differential pressure obtained by subtracting the final pressure generated by air flow in the soil from the initial atmospheric pressure. The $k_a$ values obtained from eq. (5) were converted into $\mu m^2$ units.

### 2.5.4. Soil density: Characterization and functioning of the pore system

Bulk density (BD) was calculated as the ratio of soil dry mass at 105 °C to the internal volume of the volumetric ring ($v_s$), and total porosity (TP) was determined by measuring the moisture content of saturated soil (Fig. 2). The volume of water ($v_a$) was calculated by assuming a density $\rho = 1000$ kg $m^{-3}$ and substituted into the following equation:

$$TP = \frac{v_a}{v_s} \quad (6)$$

The air-filled porosity (ε) at each matric potential was also determined. The porosity of the soil macropore domain [$MAC_{(300)}$, $m^3\ m^{-3}$] was calculated from the aeration porosity at –1 kPa, microporosity (MIC, $m^3\ m^{-3}$) as the volumetric water content of the soil at –6 kPa, and macroporosity [$MAC_{(50)}$, $m^3\ m^{-3}$] as the difference between TP and MIC (Reynolds et al., 2009) (Fig. 2).

The equivalent pore diameter at each matric potential was calculated from the capillarity equation (Libardi, 2016) and found to be>300, 100, 50, 30, 8.5, 3, and 0.6 μm at –1, –3, –6, –10, –33, –100, and –500 kPa, respectively.

The equivalent pore diameter for the soil macropore domains $MAC_{(300)}$ (–1 kPa), $MAC_{(50)}$ (–6 kPa) and MIC was 300, 50 and < 50 μm, respectively.

The $k_a$ and Ɛ values previously obtained at each matric potential

were used for indirect calculation of the geometric characteristics related to level of -organization and connectivity of the air-filled pore space ($k_1 = k_a/\varepsilon$) and ($k_2 = k_a/\varepsilon^2$) (Groenevelt et al., 1984). Since $k_1$ and $k_2$ were associated with the equivalent pore diameter at each matric potential, for example, $k_{1(300)}$ and $k_{2(300)}$ are indicators of how gas-filled pores (with an equivalent diameter > 300 μm) are organized and connected in the pore system of the soil (Poulsen, 2013).

Overall pore continuity ($N_{cont}$) was calculated by linear regression of the relation between soil permeability to air ($k_a$) and ε (Ball et al., 1988; Poulsen, 2013):

$$\log k_a = \log M + N \cdot \log \varepsilon \quad (7)$$

where $N$, called $N_{cont}$ here, is the angular coefficient of linear regression and a measure of overall pore continuity —the higher $N_{cont}$, the greater pore continuity (Ball et al., 1988). The linear regression coefficient $M$, which is designated $\varepsilon_b$ here, represents the blocked porosity to aeration (i.e., pores not contributing to convective air flow), the proportion of which was calculated as follows (Ball et al., 1988):

$$\varepsilon_b = 10^{(-\log M)/N} \times 100 \quad (8)$$

Plant-available water capacity (PAWC, mm), which is a measure of water storage, was calculated as the difference between the volumetric water content ($m^3\ m^{-3}$) at field capacity (matric potential –10 kPa) and that at the permanent wilting point (–1500 kPa), multiplied by the depth (mm) of the soil layer (Reynolds et al., 2009).

### 2.6. Micromorphological analysis

After the physical-hydraulic analyses, but before the samples were oven-dried, one sample per treatment and soil layer was subjected to micromorphological analysis (Cooper et al., 2018; Teixeira et al., 2017) to obtain qualitative information about particle arrangement and pore characteristics (Cooper et al., 2018). For this purpose, undeformed soil samples contained in the volumetric rings were air-dried to a constant weight for 30 days and then in a forced ventilation oven at 40 °C for a further 48 h. Next, the samples were removed from the rings and embedded in blue orthophthalic resin to preserve the original soil structure. Finally, thin (0.3 mm) sections obtained according to Cooper et al. (2018) and Teixeira et al. (2017) were analyzed in terms of pore morphology and various characteristics (de Castro, 2008).

To better expose the effects of APBIs on the organization and functioning of the pore system in the surface and subsurface soil layer, the previously determined physical-hydraulic attributes were classified into three groups, namely:

(a) General properties of the pore system as defined by soil mass–volume relationships and including bulk density (BD), total porosity (TP), porosity of the macropore domain [$MAC_{(300)}$], macroporosity [$MAC_{(50)}$], microporosity (MIC), soil water retention curve (SWRC), and micromorphological characteristics.
(b) Properties associated with the ability of the pore system to conduct air and water, which is governed by dynamic variables including saturated hydraulic conductivity ($k_{sat}$), and intrinsic permeability to air ($k_a$) and water ($k_w$).
(c) Continuity of soil pores, water availability to plants and root-related properties, which depend on soil attributes such as continuity($N_{cont}$), geometric characteristics related to level of -organization and connectivity-of the air-filled pore space ($k_1$ and $k_2$), blocked porosity ($\varepsilon_b$), and various other variables associated with plant-available water capacity (PAWC) and root density (RD).

### 2.7. Statistical analyses

The experimental results were checked for normality and variance homoscedasticity with the Shapiro–Wilk and Levene's test, respectively. When necessary, data were transformed for better fitting to a normal (Gaussian) distribution. All soil attributes related to water and air flows were log transformed.

The effects of the cropping systems (APBIs) on the soil parameters of each of the three groups of physical-hydraulic attributes, and their differences between the surface and subsurface layer, were assessed by factorial multivariate analysis of variance (MANOVA) with Wilks' lambda test ($p < 0.05$).

The effects of APBIs on each soil parameter in the surface and subsurface soil layer were assessed by ANOVA. The differences in each soil parameter between the surface and subsurface layer were assessed by factorial ANOVA with soil layer as one of the factors.

When the ANOVAs were significant ($p < 0.05$), the soil parameters for the surface and subsurface layer were subjected to orthogonal contrast analysis ($t$-test, $p < 0.05$) in order to assess the influence of APBIs from the different cropping systems. The contrasts were defined as follows:

- C1. Very low (BS) vs increasing APBIs (O/M, O + V/M and O + V/M + C).
- C2. Very low (BS) vs very high APBIs from pasture (PAST).
- C3. Low (O/M) vs high APBIs (O + V/M + C) from the cropping systems.

The ANOVAs and contrast analyses were performed with the software SPSS v. 21 (Norris et al., 2014). The relationship of APBIs with soil parameters (SOC, TP, MIC, $N_{cont}$, and PAWC) was assessed through the significance of Pearson's coefficient as determined by regression analysis with SigmaPlot v. 12.0.

## 3. Results

### 3.1. Active plant biomass inputs (APBIs)

The historical dataset (34 years) revealed large differences in APBIs among no-till cropping systems, with values 5.1 to 11.4 times greater than in BS (Fig. 1). APBIs ranged from 0.13 kg $m^{-2}$ $yr^{-1}$ (i.e., very low) in BS with a few weeds growing, through 0.66 kg $m^{-2}$ $yr^{-1}$ (low) with two (O/M), three (O + V/M), or four species (O + V/M + C) each year, to 1.10 kg $m^{-2}$ $yr^{-1}$ (high). Perennial pasture (PAST) supplied 1.48 kg $m^{-2}$ $yr^{-1}$ (i.e, a very high APBI) with a single species —which, however, grew throughout the year and at especially high rates in the spring/summer period.

Table 2 shows the average value for each physical-hydraulic parameter in each cropping system and soil layer. Parameters such as $k_a$, $k_{sat}$, $k_1$, and $k_2$ exhibited a high variability, however.

The MANOVA results revealed that the three groups of physical-hydraulic parameters differed highly significantly ($p < 0.001$) between the surface and the subsurface soil layer. Such parameters were associated with (1) porosity; (2) air and water flows; and (3) continuity of the pore network, water availability for plants and root growth. Also, with the exception of group (2) ($p < 0.052$), the parameters differed significantly ($p < 0.05$) between APBI levels (Table 3).

The ANOVA applied to the results for the surface and subsurface layer of the soil showed some physical-hydraulic parameters to differ between APBI levels (Table 3). Differences in TP, MIC, $k_{2(06)}$, $N_{cont}$, εb, and SOC were significant ($p < 0.05$) in the surface layer, as were those in BD, $MAC_{(300)}$, $k_{a(300)}$, $k_{sat}$ and $k_w$ in the subsurface layer. On the other hand, all parameters except $k_{a(300)}$, $k_{1(50)}$ and $k_{1(06)}$ differed significantly between the surface and subsurface soil layer ($p < 0.01$; Table 3).

### 3.2. General attributes of the pore system in the surface and subsurface layer

As can be seen from Table 3, TP and MIC in the surface layer, and BD

**Table 2**
Mean values ($n$ = 9, ± SD) of general attributes related to the soil pore system; water and air fluxes; and pore continuity, plant-available water capacity, and root density, in the surface (0–5 cm) and subsurface layer (5–15 cm) of a sandy clay loam Acrisol under no-till with variable active plant biomass inputs (APBI) for 34 years.

| Soil attribute | Cropping system: Very low APBIs BS | | Low APBIs O/M | | Medium APBIs O + V/M | | High APBIs O + V/M + C | | Very high APBIs PAST | |
|---|---|---|---|---|---|---|---|---|---|---|
| | surface | subsurface | surface | subsurface | surface | subsurface | surface | subsurface | surface | subsurface |
| ***General attributes of the soil pore system*** | | | | | | | | | | |
| **BD** | 1.54 (±0.07) | 1.68 (±0.04) | 1.56 (±0.09) | 1.77 (±0.05) | 1.5 (±0.06) | 1.69 (±0.04) | 1.39 (±0.06) | 1.7 (±0.05) | 1.46 (±0.18) | 1.76 (±0.04) |
| **TP** | 0.44 (±0.01) | 0.37 (±0.02) | 0.46 (±0.01) | 0.36 (±0.02) | 0.47 (±0.02) | 0.37 (±0.02) | 0.5 (±0.02) | 0.38 (±0.03) | 0.49 (±0.02) | 0.36 (±0.02) |
| **$MAC_{(300)}$** | 0.06 (±0.01) | 0.03 (±0.01) | 0.07 (±0.01) | 0.04 (±0.01) | 0.07 (±0.01) | 0.03 (±0.01) | 0.08 (±0.02) | 0.03 (±0.01) | 0.09 (±0.03) | 0.03 (±0.00) |
| **$MAC_{(50)}$** | 0.17 (±0.01) | 0.1 (±0.00) | 0.15 (±0.03) | 0.09 (±0.02) | 0.16 (±0.01) | 0.08 (±0.02) | 0.19 (±0.03) | 0.1 (±0.02) | 0.15 (±0.04) | 0.07 (±0.02) |
| **MIC** | 0.26 (±0.02) | 0.27 (±0.02) | 0.31 (±0.02) | 0.28 (±0.01) | 0.31 (±0.02) | 0.29 (±0.01) | 0.32 (±0.01) | 0.28 (±0.02) | 0.34 (±0.02) | 0.3 (±0.01) |
| ***Attributes related to water and air fluxes*** | | | | | | | | | | |
| **$^{*}k_{a(300)}$** | 0.6 (±0.2) | 0.7 (±0.3) | 0.8 (±0.6) | 0.6 (±0.3) | 0.5 (±0.1) | 0.6 (±0.3) | 0.6 (±0.2) | 0.9 (±0.3) | 1.1 (±0.2) | 1.4 (±0.6) |
| **$^{*}k_{a(50)}$** | 1.5 (±0.3) | 1.2 (±0.3) | 1.4 (±0.4) | 1.2 (±0.2) | 1.4 (±0.0) | 0.8 (±0.2) | 1.5 (±0.2) | 1.1 (±0.18) | 1.7 (±0.4) | 1.1 (±0.2) |
| **$^{*}k_{a(0.6)}$** | 1.9 (±0.0) | 2 (±0.2) | 2.0 (±0.1) | 1.8 (±0.3) | 2.0 (±0.0) | 1.6 (±0.2) | 2 (±0.1) | 1.8 (±0.1) | 2.1 (±0.3) | 2.0 (±0.2) |
| **$^{*}k_{sat}$** | 2.1 (±0.2) | 0.7 (±0.4) | 1.4 (±0.7) | 1.5 (±0.1) | 2 (±0.1) | 0.8 (±0.3) | 2.2 (±0.1) | 1.7 (±0.1) | 2.2 (±0.7) | 1.5 (±0.4) |
| **$k_w$** | 4.0 (±1.7) | 0.2 (±0.1) | 1.7 (±2.4) | 1 (±0.3) | 3 (±0.4) | 0.2 (±0.1) | 5 (±1.6) | 1.4 (±0.2) | 10 (±11.9) | 1.3 (±0.9) |
| ***Attributes related to organization in soil pores, plant-available water capacity, roots and soil organic carbon*** | | | | | | | | | | |
| **$^{*}k_{1(300)}$** | 1.8 (±0.2) | 2.1(±0.2) | 1.9 (±0.5) | 2.1 (±0.2) | 1.7 (±0.2) | 2.1 (±0.3) | 1.7 (±0.2) | 2.4 (±0.2) | 2.2 (±0.4) | 2.6 (±0.1) |
| **$^{*}k_{1(50)}$** | 2.3 (±0.2) | 2.2 (±0.2) | 2.2 (±0.3) | 2.1 (±0.1) | 2.2 (±0.0) | 1.9 (±0.1) | 2.2 (±0.1) | 2.2 (±0.1) | 2.4 (±0.2) | 2.3 (±0.1) |
| **$^{*}k_{1(0.6)}$** | 2.5 (±0.0) | 2.7 (±0.1) | 2.6 (±0.1) | 2.6 (±0.3) | 2.6 (±0.0) | 2.4 (±0.2) | 2.7 (±0.0) | 2.5 (±0.1) | 2.8 (±0.3) | 2.8 (±0.1) |
| **$^{*}k_{2(300)}$** | 3.1 (±0.1) | 3.7 (±0.4) | 3.1 (±0.5) | 3.5 (±0.2) | 2.9(±0.2) | 3.7 (±0.3) | 2.8 (±0.2) | 4 (±0.2) | 3.3 (±0.3) | 4.2 (±0.2) |
| **$^{*}k_{2(50)}$** | 3.1 (±0.2) | 3.2 (±0.2) | 3.0 (±0.2) | 3.2 (±0.1) | 3 (±0.0) | 3.1 (±0.0) | 2.9 (±0.1) | 3.4 (±0.3) | 3.2 (±0.2) | 3.5 (±0.0) |
| **$^{*}k_{2(0.6)}$** | 3.1 (±0.1) | 3.5 (±0.1) | 3.2 (±0.0) | 3.5 (±0.3) | 3.2 (±0.1) | 3.2 (±0.2) | 3.3 (±0.1) | 3.3 (±0.1) | 3.5 (±0.2) | 3.6 (±0.0) |
| **$N_{cont}$** | 1.8 (±0.1) | 1.8 (±0.25) | 2.3 (±0.3) | 2.2 (±0.2) | 2.1 (±0.3) | 1.3 (±0.2) | 2.5 (±0.28) | 1.1 (±0.52) | 2 (±0.2) | 1 (±0.3) |
| **$\varepsilon_b$** | 2.0 (±0.5) | 2 (±0.92) | 4 (±0.8) | 2 (±0.3) | 3 (±1.0) | 2 (±0.4) | 5 (±0.6) | 1 (±0.7) | 3 (±1.1) | 0.3 (±0.4) |
| **PAWC** | 7.0 (±1.0) | 11 (±1.88) | 8 (±1.1) | 13 (±1.0) | 9 (±1.2) | 14 (±0.7) | 8 (±0.2) | 13 (±2.1) | 10 (±0.9) | 14 (±1.1) |
| **RD** | 1.7 (±0.4) | 0.4 (±0.1) | 0.7 (±0.6) | 0.1 (±0.4) | 1.6 (±0.3) | 0.3 (±0.0) | 0.9 (±0.4) | 0.2 (±0.0) | 1.8 (±2.0) | 1.3 (±1.2) |
| **SOC** | 12 (±1.1) | 8 (±0.6) | 13 (±0.8) | 8 (±0.3) | 16 (±0.7) | 9 (±1.3) | 17 (±1.2) | 10 (±0.4) | 17 (±1.7) | 9 (±0.2) |

BS, bare soil (APBIs = 0.13 kg DM $m^2$ $year^{-1}$); PAST, perennial pasture (APBIs = 1.48 kg DM $m^2$ $year^{-1}$); O/M, oat/maize (APBIs = 0.66 kg DM $m^2$ $year^{-1}$); O + V/M, oat + vetch/maize (APBIs = 0.93 kg DM $m^2$ $year^{-1}$); O + V/M + C, oat + vetch/maize + cowpea (APBIs = 1.10 kg DM $m^2$ $year^{-1}$); BD (Mg $m^{-3}$), bulk density; TP ($m^3$ $m^{-3}$), soil total porosity; $MAC_{(300)}$ ($m^3$ $m^{-3}$), porosity of soil macropore domain; $MAC_{(50)}$ ($m^3$ $m^{-3}$), soil macroporosity; MIC ($m^3$ $m^{-3}$), soil microporosity; * values expressed in Log (10); $k_{a(300)}$, $k_{a\ (50)}$, $k_{a\ (0.6)}$ ($\mu m^2$), soil intrinsic permeability to air in pores with equivalent diameter > 300, > 50, and > 0.6 μm, respectively; $k_{sat}$ (mm $h^{-1}$), saturated hydraulic conductivity; $k_w$ ($\mu m^2$), soil intrinsic permeability to water; $k_{1(300)}$, $k_{1(50)}$, $k_{1(0.6)}$ ($\mu m^2$ $m^{-3}$ $m^3$), pore organization indices with equivalent diameter > 300, > 50, and > 0.6 μm, respectively; $k_{2(300)}$, $k_{2(50)}$, $k_{2(0.6)}$ [$\mu m^2$ ($m^{-3}$ $m^3$)$^2$], pore organization indices with equivalent diameter > 300, > 50, and > 0.6 μm, respectively; $N_{cont}$, overall pore continuity; $\varepsilon_b$ (%), blocked porosity to aeration; PAWC (mm), plant-available water capacity; RD (g $kg^{-1}$), root density; SOC (g $kg^{-1}$) Soil Organic Carbon. $MAC_{(300)}$: critical ≤ 0.04 $m^3$ $m^{-3}$, Good: ≥ 0.07 $m^3$ $m^{-3}$; and **$MAC_{(50)}$** good: ≥ 0.1 $m^3$ $m^{-3}$ (Reynolds et al., 2009). **BD**: critical > 1.67 Mg $m^{-3}$ (Reichert et al., 2009).

and $MAC_{(300)}$ in subsurface layer, were the individual parameters most strongly influenced by APBI level. Also, the results confirmed the marked differences in pore system between the two layers ($p < 0.001$; Table 3, Fig. 4). Thus, TP and MIC in the surface layer averaged at 0.44–0.5 and 0.26–0.34 $m^3$ $m^{-3}$, respectively, with high and very high APBI levels (O + V/M + C, PAST) exhibiting the highest averages. TP and MIC in the subsurface layer averaged at 0.36–0.38 and 0.27–0.30 $m^3$ $m^{-3}$, respectively. Therefore, TP and MIC were 22 and 8 % lower in the subsurface layer than they were in the surface layer (Table 2).

BD in the subsurface soil layer ranged from 1.68 to 1.77 Mg $m^{-3}$ and peaked with O/M and PAST. This parameter was 15 % higher on average in the subsurface layer. Also, $MAC_{(300)}$ was 33 % greater with the O/M treatment than with the others (Table 2).

The contrast analysis showed that increasing APBIs in no-till soil (BS vs O/M, O + V/M and O + V/M + C − Contrast C1, and BS vs PAST – Contrast *C*2) increased TP in the surface soil layer by 8 and 11 %, respectively, relative to very low APBI levels (BS). MIC in that layer was 23 and 31 % with high (O + V/M + C) and very high (PAST) APBIs, respectively, relative to BS [p < 0.001; Table 2, Table 4 (C1, *C*2), Fig. 4].

APBIs affected BD differently. Based on the C3 contrast, the cropping system comprising four species (O + V/M + C) significantly decreased BD relative to the cropping system involving only two species (O/M): from 1.56 to 1.39 Mg $m^{-3}$ in the surface soil layer and 1.8 to 1.7 Mg $m^{-3}$ in the subsurface layer ($p < 0.05$; Table 2, Table 4 (C3)]. In the *C*2 contrast, PAST significantly increased BD in the subsurface soil layer: from 1.68 to 1.76 Mg $m^{-3}$ [$p < 0.05$; Table 2, Table 4 (*C*2)].

Applying the bimodal model of Seki (2007) to the results revealed differences in SWRC between cropping systems (Fig. 3). In the surface soil layer, PAST, O + V/M + C, and O + V/M differed in SWRC from BS at matric potentials from 0 to –60 hPa and –60 hPa to –10000 hPa, the two curve segments being primarily governed by $MAC_{(50)}$ and MIC, respectively. In the subsurface soil layer, the curves discriminated between O + V/M and PAST at matric potentials from –60 to –5000 hPa, a range governed by MIC (Fig. 3).

The micromorphological images of the surface and subsurface layers revealed the presence of channels, biopores, and fissures forming a complex network of interconnected pores (blue in the micromorphological sheets, Fig. 3). Based on the images, the pore network expanded in response to the gradient of APBIs in both soil layers. Also, the effects of high (O + V/M + C) and very high APBIs (PAST) on the pore network were more apparent in the surface soil layer than they were in the subsurface layer.

### 3.3. Capacity of the pore system to conduct air and water

As can be seen from Table 3, the water conduction characteristics of pore system also differed markedly between soil layers. Differences in the capacity of the pore system to conduct air and water between APBI levels were significant ($p < 0.05$) but only in the subsurface layer (Table 3).

**Table 3**
Summary of results of statistical analysis on the long-term effect (34 yr) of no-till cropping systems on attributes of the soil pore system in the surface (0–5 cm) and subsurface layer (5–15 cm) of a subtropical sandy clay loam Acrisol.

| Statistical test Soil Parameter | MANOVA (Wilks' lambda) | | | ANOVA | | |
|---|---|---|---|---|---|---|
| | Cropping system (APBIs) | Soil layers (L) | APBIs × L | APBIs surface | APBIs subsurface | Soil layer (L) |
| | *p* | *p* | *p* | *p* | *p* | *p* |
| | | | ***General attributes of the soil pore system*** | | | |
| **BD** | **0.018** | **< 0.0001** | 0.446 | 0.293 | **0.029** | **<0.000** |
| **TP** | | | | **0.009** | 0.888 | **<0.000** |
| **$MAC_{(300)}$** | | | | 0.450 | **0.031** | **<0.000** |
| **$MAC_{(50)}$** | | | | 0.496 | 0.171 | **<0.000** |
| **MIC** | | | | **0.007** | 0.204 | **<0.000** |
| | | | ***Attributes related to water and air fluxes*** | | | |
| **$k_{a(300)}$** | 0.052 | **< 0.0001** | **0.015** | 0.235 | **0.047** | 0.477 |
| **$k_{a(50)}$** | | | | 0.803 | 0.205 | **0.0035** |
| **$k_{a(0.6)}$** | | | | 0.687 | 0.158 | **0.044** |
| **$k_{sat}$** | | | | 0.270 | **0.009** | **<0.000** |
| **$k_w$** | | | | 0.532 | **0.026** | **0.015** |
| | | | ***Attributes related to organization in soil pores, plant-available water capacity, roots and soil organic carbon*** | | | |
| **$k_{1(300)}$** | **0.002** | **<0.0001** | **0.036** | 0.191 | **0.041** | **0.001** |
| **$k_{1(50)}$** | | | | 0.657 | *0.051* | 0.142 |
| **$k_{1(0.6)}$** | | | | 0.102 | 0.101 | 0.694 |
| **$k_{2(300)}$** | | | | 0.147 | **0.045** | **<0.001** |
| **$k_{2(50)}$** | | | | 0.216 | 0.128 | **<0.001** |
| **$k_{2(0.6)}$** | | | | **0.039** | **0.036** | **0.004** |
| **$N_{cont}$** | | | | **0.021** | **0.010** | **<0.001** |
| **$\varepsilon_b$** | | | | **0.024** | **0.020** | **<0.001** |
| **PAWC** | | | | 0.106 | 0.081 | **<0.001** |
| **RD** | | | | 0.390 | 0.204 | **0.004** |
| **SOC** | | | | **0.004** | **0.01** | **<0.001** |

BD (Mg $m^{-3}$), bulk density; TP ($m^3 m^{-3}$), soil total porosity; $MAC_{(300)}$ ($m^3 m^{-3}$), porosity of soil macropore domain; $MAC_{(50)}$ ($m^3 m^{-3}$), soil macroporosity; MIC ($m^3 m^{-3}$), soil microporosity; $k_{a(300)}$, $k_{a(50)}$, $k_{a(0.6)}$ ($\mu m^2$) soil intrinsic permeability to air in pores with equivalent diameter > 300, > 50, and > 0.6 μm, respectively; $k_{sat}$ (mm $h^{-1}$), saturated hydraulic conductivity; $k_w$ ($\mu m^2$), soil intrinsic permeability to water; $k_{1(300)}$, $k_{1(50)}$, $k_{1(0.6)}$ ($\mu m^2$ $m^{-3}$ $m^3$), pore organization indices with equivalent diameter > 300, > 50, and > 0.6 μm, respectively; $k_{2(300)}$, $k_{2(50)}$, $k_{2(0.6)}$ [$\mu m^2$ ($m^{-3}$ $m^3$)$^2$], pore organization indices with equivalent diameter > 300, > 50, and > 0.6 μm, respectively; $N_{cont}$, overall pore continuity; $\varepsilon_b$ (% v/v), blocked porosity to aeration; PAWC (mm), plant-available water capacity; RD (g $kg^{-1}$), root density; and SOC (g $kg^{-1}$) Soil Organic Carbon.

The permeability to air, $k_a$, ranged from 0.5 to 2.1 $\mu m^2$ (in log units) and 0.6 to 2 $\mu m^2$ in the subsurface soil layer (Table 2). Also, $k_{a(300)}$ in the subsurface soil layer differed significantly between APBI levels, with values ranging from 0.6 to 1.4 $\mu m^2$ ($p < 0.05$; Table 2).

Air flow in macropores [$k_{a(50)}$] and micropores [$k_{a(06)}$] was 27 and 8 % lower, respectively, in the subsurface soil layer (Table 2). Water fluxes as measured in terms of saturated hydraulic conductivity ($k_{sat}$) and intrinsic permeability to water ($k_w$) averaged at 0.7–1.7 mm mm $h^{-1}$ (in log units) and < 0.01–0.1 $\mu m^2$, respectively, in the subsurface layer (Table 2). Finally, the water flux-related parameters $k_{sat}$ and $k_w$ were 36 and 83 % lower, respectively, on average in the subsurface layer (Table 2).

The contrast analyses revealed that the set of cropping systems (low, medium and high APBIs) [Table 4 (C1)], and the very high APBIs [Table 4 (*C2*)] significantly increased the capacity of pores to conduct water in the subsurface soil layer ($k_{sat}$, $k_w$) relative to BS: by 84 and 114 %, respectively ($p < 0.05$; Tables 2 and 4). As revealed by *C2*, air permeability in $k_{a(300)}$ macropores in PAST was twice higher than in BS (Table 4).

### 3.4. Pore system organization, available water, and root density

The geometrical indices related to level of organization and connectivity of the air-filled macropores [$k_{1(300)}$ and $k_{2(300)}$] differed significantly between APBI levels but only in the subsurface soil layer ($p < 0.05$; Table 3). By contrast, geometrical indices of air-filled micropores [$k_{2(0.6)}$], overall pore continuity ($N_{cont}$) and air-blocked porosity ($\varepsilon_b$) differed in both the surface and the subsurface layer ($p < 0.05$; Table 3, Fig. 4). The differences between the two layers occurred in all parameters relating to pore system organization except $k_{1(50)}$ and $k_{1(06)}$ ($p < 0.01$; Table 3, Fig. 4).

Pore organization and connectivity indices ($k_1$ and $k_2$) by 300 to 0.6 μm diameter range in the surface soil layer increased as the soil samples were drained. In the subsurface it was different for the parameter $k_2$ over the previous diameter range. In BS, O + V/M + C, and PAST $k_2$ decreased 5.4, 17.5 and 14.3 %, respectively (Table 2).

$k_{1(300)}$ and $k_{2(300)}$ averaged at 2.1–2.6 $\mu m^2$ $m^{-3}$ $m^3$ and 3.5–4.2 $\mu m^2$ ($m^{-3}$ $m^3$)$^2$, respectively, in the subsurface soil layer (Table 2). Overall pore continuity ($N_{cont}$) and air-blocked porosity ($\varepsilon_b$) spanned the range 1.8–2.5 and 2–5 %, respectively, in the surface layer, and 1.1–2.2 and 0.3–2 %, respectively, in the subsurface layer (Table 2).

As regards cropping systems, PAWC in the surface soil layer accounted for 7–10 mm of available water, and RD ranged from 0.7 to 1.8 g roots $kg^{-1}$ soil. In the subsurface soil layer, PAWC was 11–14 mm and RD 0.1–1.3 g roots $kg^{-1}$ soil (Table 2).

The contrast analyses revealed that $N_{cont}$ and $\varepsilon_b$ in the surface soil layer increased by 28–100 % relative to BS with increasing APBI in all cropping systems [$p < 0.05$; Table 2, Table 4 (C1)]. As can be seen in Fig. 4, the relationship was linear. The very high APBI levels of PAST significantly increased pore organization and connectivity in micropores [$k_{2(0.6)}$] relative to BS: by 16 % [($p < 0.02$; Table 2, Table 4 (*C2*)].

In the subsurface soil layer, PAST significantly increased $k_{1(300)}$ and $k_{2(300)}$ relative to BS: by approximately 24 and 13,5%, respectively [$p < 0.05$; Table 2, Table 4 (*C2*)]. By contrast, in subsurface layer, PAST and O + V/M + C significantly ($p < 0.01$) decreased $N_{cont}$ and $\varepsilon_b$ relative to BS: by 44, 85 %, respectively (Table 4, *C2*) and relative to O/M: by 52 and 50 % respectively (Table 4, C3) (Tables 2 and 4, Fig. 4). PAWC increased by 21 % ($p < 0.05$) with increasing APBI in the annual cropping systems [O/M, O + V/M, O + V/M + C; Table 4 (C1), Table 2]. Also, perennial pasture increased PAWC by 27 % [Table 4, Table 2 (*C2*)]. PAWC was linearly related to the APBIs supplied by the cropping systems (Fig. 4).

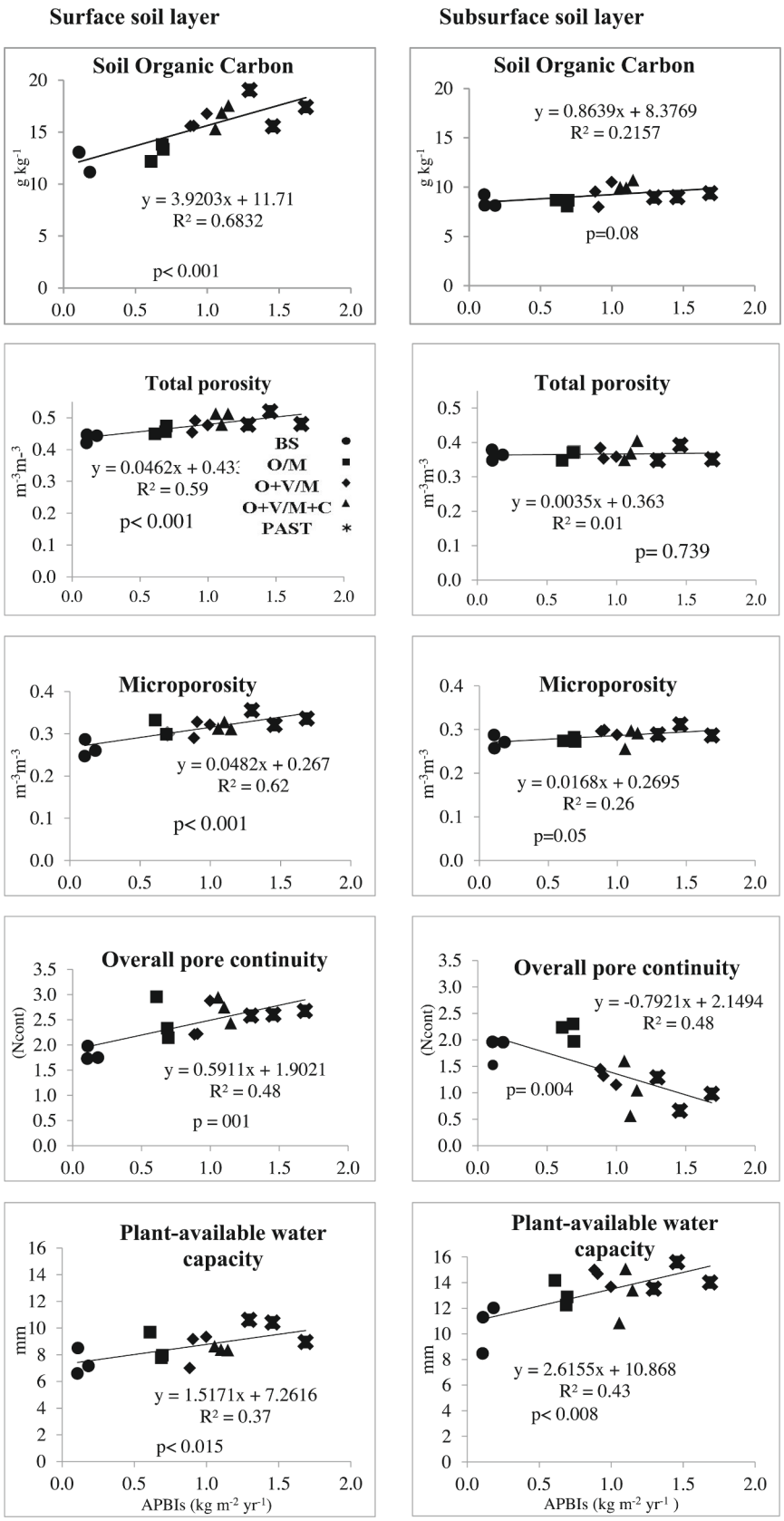


**Fig. 4.** Relationship between characteristics of the soil pore system in the surface (0–5 cm) and subsurface layer (5–15 cm) of a subtropical Acrisol and active plant biomass inputs (APBIs) from plants in different no-till cropping systems: BS, bare soil; PAST, perennial pasture; O/M, oat/maize; O + V/M, oat + vetch/maize; and O + V/M + C, oat + vetch/maize + cowpea. Each of the three points represents one of the blocks evaluated in the experiment. The value for each block was obtained from $n = 9$ evaluations conducted over the 34 years of the experiment.

**Table 4**
Summary of results of the contrast analysis between no-till cropping systems and changes in attributes of the soil pore system in the surface (0–5 cm) and subsurface layer (5–15 cm) of a subtropical sandy clay loam Acrisol.

| Contrast | C1<br>BS vs (O/M, O + V/M, O + V/M + C) | C2<br>BS vs PAST | C3<br>O/M vs O + V/M + C |
|---|---|---|---|
| | ***General attributes of the soil pore system*** | | |
| **Surface** | TP **↑<br>MIC **↑ | TP **↑<br>MIC **↑ | BD *↓<br>TP *↑ |
| **Subsurface** | | BD *↑ | BD *↓ |
| | ***Attributes related to water and air fluxes*** | | |
| **Subsurface** | $k_{sat}$ **↑<br>$k_w$ *↑ | $k_{sat}$ **↑ $k_w$ *↑<br>$k_{a(300)}$ *↑ | |
| | ***Attributes related to organization in soil pores, plant-available water capacity, and roots*** | | |
| **Surface** | $N_{cont}$ *↑<br>$\varepsilon_b$ *↑ | $k_{2(0.6)}$ **↑ | |
| **Subsurface** | PAWC *↑ | $k_{1(300)}$ *↑<br>PAWC #↑<br>$k_{2(300)}$ *↑<br>$N_{cont}$ ** ↓<br>$\varepsilon_b$ *↓ | $N_{cont}$ **↓<br>$\varepsilon_b$ **↓ |

BS, bare soil; PAST, perennial pasture; O/M, oat/maize; O + V/M, oat + vetch/maize; O + V/M + C, oat + vetch/maize + cowpea; TP, soil total porosity; MIC, soil microporosity; BD, bulk density; $k_{sat}$, saturated hydraulic conductivity; $k_w$, soil intrinsic permeability to water; $k_{1(300)}$, organization index in pores with equivalent diameter > 300, respectively; $k_{2(300)}$, $k_{2(0.6)}$ [$\mu m^2$ ($m^{-3}$ $m^3$)$^2$], organization indices in pores with equivalent diameter > 300,and > 0.6 μm, respectively; $N_{cont}$, overall pore continuity; $\varepsilon_b$, blocked porosity to aeration; PAWC, plant-available water capacity; RD, root density. Up- and down-pointing arrows indicate an increase or decrease, respectively, from the first to the second component (cropping systems) in each contrast. Statistical significance: # $p < 0.1$,* $p < 0.05$, ** $p < 0.001$.

Soil organic carbon (SOC) was also dependent on APBI level, and on the soil surface and subsurface conditions ($p < 0.01$; Table 3). Thus, SOC was 12–17 g $kg^{-1}$ in the subsurface soil layer but lower (8–10 g $kg^{-1}$) in the surface layer. Overall, average SOC values were 41 % higher in the surface layer than they were in the subsurface layer.

Fig. 4 illustrates the effects of APBIs on pore attributes such as TP, MIC, $N_{cont}$, PAWC, and SOC in the two soil layers. Plants affected the pore system and SOC in the two layers differently. Thus, they increased SOC, TP, MIC, $N_{cont}$, in the surface layer, but only MIC and PAWC in the subsurface layer —where $N_{cont}$ was decreased and total porosity unaffected (Fig. 4).

## 4. Discussion

### 4.1. Active plant biomass inputs (APBIs) and changes in the soil pore system

The results of the ANOVA (Table 3), contrast analysis (Table 4) and regression analysis (Fig. 4) exposed the long-term effects (34 years) of APBI gradients on no-till soil in the target subtropical ecosystem. The effects on the pore system and SOC were especially apparent in both the surface (0–5 cm) and the subsurface soil layer (5–15 cm) (Table 4, Fig. 4). This result confirms that no-till soils must be cropped with a large number of annual or perennial species in order to maintain functional porosity so as to allow growing plants to ensure adequate soil energy and C fluxes. APBIs from plants impacted soil parameters associated to the pore system, water and air fluxes; also, they related to continuity in soil pores and to SOC (Tables 3 and 4; Fig. 4).

#### 4.1.1. Effects of APBIs on the soil pore system in the surface layer

Based on the results for the surface soil layer and, especially, the increased porosity and continuity of pore system (TP, MIC, $N_{cont}$), and organization/connectivity in micropores [$k_{2(0.6)}$] (Table 3, Table 4, Fig. 4), APBIs helped construct a pore system that facilitated water storage and gas exchange. The presence of channels, biopores, and fissures resulting from root growth, in conjunction with soil biota, facilitated the formation of a highly complex pore network in the soil surface layer (Fig. 3). These soil conditions ensure effective water infiltration, and also efficient air and water conduction to subsurface soil (Pires et al., 2017; Rabot et al., 2018; Weiler and Naef, 2003).

Roots were previously found to facilitate the formation of large, functional pores called “biopores” in legume- and grass-bearing systems compared to bare soil (Carof et al., 2007; Obi, 1999). According to Fischer et al. (2015), and Weisser et al. (2017), soil porosity is affected by plant diversity and soil biota. This was very consequential for our results since Almeida et al. (2016) detected an impact of no-till cropping systems on two Isoptera groups (termites), which are known to influence the formation of pore networks by connecting cavities and vesicles in the soil surface (Barros et al., 2000).

Plant–biota interactions in the studied no-till soil were confirmed by micromorphological analyses (Fig. 3), which revealed a prevalence of fine to medium macropores (0.75 to > 2 mm in diameter) of primarily biological origin (de Castro, 2008) as result of the combined action of roots and soil biota (Cooper et al., 2018; Pires et al., 2017), and of increasing APBI levels. In the surface, the pore system promotes capturing, conduction and storage of resources such as water. This role of the pore system can be interpreted as one of the results of self-organization in no-till soils under the influence of growing plants (Fig. 5). Thus, the presence of growing plants increases energy and matter inputs, thus increasing pore connectivity ($N_{cont}$) and helping develop a micropore network highly organized [$k_{2(0.6)}$], all of which facilitates storage of available water for use by plants and soil biota (Vezzani and Mielniczuk, 2011a), and boosts biogeochemical processes as a result (Smucker et al., 2007).

SWRC (Fig. 3) was also consistent with a pore system that facilitated water storage and gas exchange, with an increased TP in the surface soil layer. The differences in SWRC were observed between the cropping systems O + V/M + C, PAST and BS, especially, both in the macropore and in the micropore range (matric potentials from 0 to − 60 and − 60 to − 10 000 hPa, respectively). These differences in SWRC were confirmed by the contrasting sinuosity between curves and quality parameters in the multimodal model of Seki (2007), $R^2 > 0.98$, and by the low dispersion of data in all curves. Therefore, multimodal SWRC models are suitable for soils with a heterogeneous pore system (Durner, 1994), which is the case with tropical soils (Omuto, 2009).

Increasing APBIs promoted retention of energy and matter in the form of soil organic carbon (Table 4). The increase in SOC can be ascribed to microbially produced organic compounds from the decomposition of plant residues covering the soil (Cotrufo et al., 2013), and also to rhizodeposition products.

#### 4.1.2. Effects of APBIs on the soil pore system in the subsurface layer

High APBI levels in the subsurface soil layer (5–15 cm) enabled the development of a pore system differing from that in the surface layer (0–5 cm). Such a system increased water fluxes ($k_{sat}$, $k_w$), decreased pore connectivity ($N_{cont}$), and increased water availability (PAWC) (Tables 3 and 4). The improved water fluxes may have resulted from the formation of an increased number of connected pores of equivalent diameter > 300 μm [$k_{1(300)}$] (Tables 3 and 4), probably by effect of root growth establishing preferential channels for water infiltration (Nicoloso et al., 2008) and of the activity of earthworms constructing continuous vertical channels (Blouin et al., 2013; Langmaack et al., 1999). Root mass in the subsurface soil layer was 3 times greater with PAST than it was with the other treatments (Table 2), which probably facilitated the development of a more continuous pore network —and hence boosted water and air

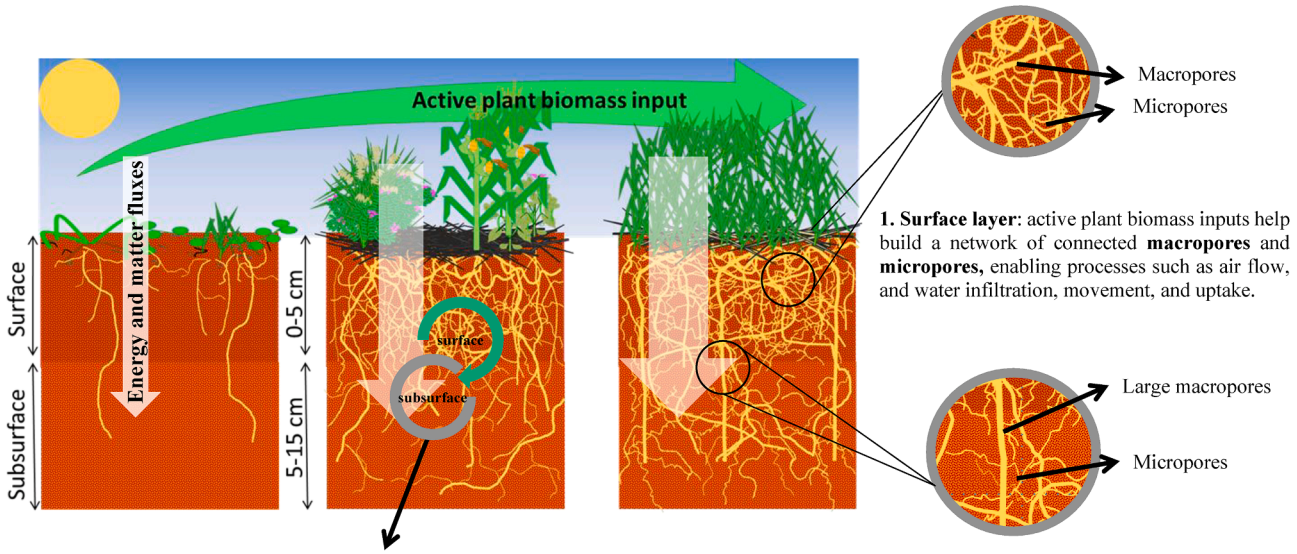


**Fig. 5.** Active plant biomass inputs affect functioning of the pore network in the surface and subsurface layers of soil.

fluxes as a result (Table 4). Some authors (e.g., Obi, 1999) have found pasture to increase $k_{sat}$ relative to bare soil, but others have not (Carof et al., 2007). According to Weisser et al. (2017), $k_{sat}$ is influenced by crop growth stage and root development; thus, a low growing root system takes little pore space and leaves many free pores that facilitate water fluxes in no-till soils. At the time of soil sampling here (late winter), when oat and vetch were senescent and PAST resulted in little plant growth, roots must have stopped growing or even died, and part of the pore space been freed, thereby boosting water fluxes in the subsurface layer as a result.

Some studies have shown that the presence of legumes in cropping systems acts as a source of nitrogen, thus promoting earthworm activity (Almeida et al., 2016) and biopore formation (Blouin et al., 2013;)—and hence increasing water fluxes (Fischer et al., 2014; Langmaack et al., 1999; Weisser et al., 2017). These conditions may have prevailed with O + V/M + C and the system promoted the formation of the many channels and connected pores observed in the micromorphological images of the subsurface soil layer (Fig. 3).

Macropore continuity in subsurface soil strongly influences water storage by facilitating water transfer from macropores to the bulk soil in no-till systems (Weiler and Naef, 2003). Based on the results, this functionality of macropores (viz., mobilizing water to the soil matrix) resulted from self-organization of the soil in the subsurface layer by effect of the plants —in fact, $k_{sat}$ and PAWC increased with increasing APBIs (Table 4, Fig. 4). The increasing PAWC values of Table 4 and Fig. 4 may have resulted from decreased $N_{cont}$ values (Fig. 4) leading to slower movement of water in the soil matrix, and hence to increased storage.

#### 4.1.3. *In what way are the pore systems in the surface and surface soil layer complementary?*

The data in Tables 3 and 4, and those in Figs. 4 and 5, strengthen our hypothesis that APBIs promote the formation of a pore network differing in their characteristics and playing complementary roles in the surface and subsurface layer of a no-till soil. The functional complementariness of the two layers is a result of the compleX arrangement and connection of macropore and micropore networks (Fig. 5). The increased continuity of the pore system in the surface layer facilitates water infiltration and storage, gas exchange, and water fluxes to deeper layers (Fig. 5). Likewise, the connected large macropores in the subsurface layer efficiently conduct water from the soil surface. The large connected pores act as bridges between the surface and subsurface soil layers (Weiler and Naef, 2003), thereby ensuring complementariness by facilitating fluxes between a soil layer largely functioning to capture and store resources including water and SOC (Table 4), and another storing such resources. Blackwell et al. (1990), Schäffer et al. (2008), and Holthusen et al. (2018), found vertically oriented biopores to be less prone to degradation —which is important for air and water conduction to the soil subsurface— and also to be facilitators of root growth in deep layers (de Moraes et al., 2018) and of soil functioning (Weiler and Naef, 2003).

### 4.2. *Functionality of the pore systems in response to crops*

The effect of APBIs on soil parameters was quite apparent from our results. The positive effect of APBIs on functionality the pore system overshadowed potentially adverse effects of machine traffic on the soil. Comparing the results for bare soil (BS, which was not subjected to machine traffic) with the set of crops used in the cropping systems (O/M, O + V/M, and O + V/M + C) the crops increased porosity TP, microporosity MIC, and air fluxes [$k_{a(0.6)}$] in the surface layer, as well as permeability to water fluxes ($k_w$) in the subsurface layer [Table 4 (C1)].

The improved functionality and quality of the pore system resulting from APBIs is apparent from the average values of $k_{a(300)}$: 4–9 $\mu m^2$ (Table 2). When the soil contained more moisture (matric potential = –1 kPa) and internal air fluxes stopped, the treatments exceeded the critical limit 1 $\mu m^2$ (Ball et al., 1988; Poulsen, 2013). Also, $k_{a(50)}$ increased to 20–34 $\mu m^2$ (Table 2) when all macropores were water-free (i.e., at a matric potential of –6 kPa). These results suggest that increased APBIs improve the quality of the pore system even with machine traffic. Some studies have found heavily restricted soil aeration in no-till soils (Betioli Junior et al., 2014; Holthusen et al., 2018). Such studies, however, were conducted in areas with a long-term use of soybean monocultures and a high frequency of winter fallow, which led to low APBIs.

The results of contrast C3 (viz., O/M vs O + V/M + C) illustrate the effects of high APBIs on the development of a better pore system

(Table 4). Although these cropping systems involved similar machine traffic, the soil exhibited smaller BD, and greater TP, under O + V/M + C than it did under O/M. The increased resistance of the pore system with O + V/M + C here may have been a consequence of the increased SOC resulting from the treatment (Fig. 4) (Veloso et al., 2020, 2019). Thus, the O + V/M + C treatment decreased BD in the soil surface by 11 %: from 1.56 Mg $m^{-3}$ in the 0–10 cm layer in 1983 (i.e., before the experiment was started; Pedó, 1986) to 1.39 Mg $m^{-3}$ in the 0–5 cm layer (Table 2). Moreover, O + V/M + C increased TP by 47 %: from 0.34 $m^3$ $m^{-3}$ (Pedó, 1986) to 0.50 $m^3$ $m^{-3}$ (Table 2).

PAST and O + V/M + C resulted in soil macropore domain values above the critical threshold [$MAC_{(300)} \leq 0.04$ $m^3$ $m^{-3}$; Reynolds et al., 2009] in the surface layer (Table 2), the increase relative to BS being 50 and 33 %, respectively. In contrast, $MAC_{(300)}$ in the subsurface layer fell below the critical threshold with all treatments. Although $MAC_{(300)}$ was below the threshold under PAST and O + V/M + C, these two treatments increased water fluxes ($k_{sat}$, $k_w$), which are $MAC_{(300)}$ -dependent, in the soil subsurface (Table 4), thus reflecting the increased organization of the pore system.

The mean BD value in the subsurface layer with PAST, 1.76 Mg $m^{-3}$, exceeded the critical threshold [viz., 1.67 Mg $m^{-3}$ as determined by Reichert et al. (2009) for a soil containing 220 g clay $kg^{-1}$]. However, extensive development of the pore system in the subsurface layer under PAST increased water conductivity ($k_{sat}$ and $k_w$); also, it increased macropore continuity [$k_{1(300)}$], and air flux in macropores [$k_{a(300)}$] [Table 4 (*C*2)], which testifies to the quality of the pore system in contrast to the potential deterioration of the soil suggested by the BD critical threshold.

Air capacity values above 0.10 $m^3$ $m^{-3}$ represent the proportion of pores at a matric potential of –10 kPa above which the susceptibility of soil to deficient aeration starts to decrease (Reynolds et al., 2009). Although $MAC_{(50)}$ was determined at a matric potential of –6 kPa —and hence in wetter soil—, here it exceeded 0.10 $m^3$ $m^{-3}$ (by a factor of up to 2 with O + V/M + C; Table 2) in the surface layer and was close to this threshold in the subsurface layer. These results suggest that the pore system in soils under no-till receiving very high (PAST) or high APBIs (O + V/M + C) enables efficient gas exchange in the rhizosphere even under wetter conditions.

## 5. Conclusions

The impact of crops on the pore system reflects the fluxes of energy and matter through active plant biomass inputs in a soil self-organizing process. Plants facilitate the development of resistant pore networks with different, complementary functions in the surface (0–5 cm) and subsurface layer (5–15 cm) of no-till soil. Increasing the input of active plant biomass (shoot biomass) by growing a large number of annual or perennial species improved total soil porosity and led to a more continuous pore system that facilitated water storage and gas exchange in the surface soil layer. Also, the action of plants in the subsurface soil layer facilitated the development of interconnected macropores that boosted water and air fluxes in the soil in addition to a less continuous network of pores which, in combination with micropores, increased water storage and availability to plants. Our results highlight the role of active plant biomass inputs in developing a soil pore system with improved functionality in no-till soils. However, the treatment design does not allow us to draw solid conclusions on the influence of species richness on the soil pore system because this parameter was analyzed together with plant biomass in cropping systems. Furthermore, the specific role of the root system in the development of the pore system should be examined in future research.

## Funding Information

This work was funded by the National Council for Scientific and Technological Development (CNPq, 141328/2016-9 and 406635/2022-6), the Research Support Foundation of Rio Grande do Sul (Fapergs, 22/2551-0000392-3), and RCGI – Research Centre for Gas Innovation, hosted by the University of São Paulo (USP) and sponsored by FAPESP – São Paulo Research Foundation (2020/15230-5) and Shell Brasil.

## Declaration of Competing Interest

The authors declare that they have no known competing financial interests or personal relationships that could have appeared to influence the work reported in this paper.

## Data availability

Data will be made available on request.

## Acknowledgments

This work was funded by the National Institute of Science and Technology for a Low Carbon Agriculture (INCT-Low Carbon Agriculture) under the sponsorship of CNPq (406635/2022-6), the Technological and Innovation Network for a Low Carbon Agriculture in South Brazil under FAPERGS (22/2551-0000392-3), and the Research Centre for Gas Innovation (RCGI) under FAPESP (2020/15230-5) and Shell Brazil. The authors thank the staff at Experimental Station of UFRGS, whose help and support were essential to maintain the long-term field experiment.

## References

Almeida, D.O., Bayer, C., Almeida, H.C., 2016. Fauna e atributos microbiológicos de um Argissolo sob sistemas de cobertura no Sul do Brasil. Pesquisa Agropecuaria Brasileira 51, 1140–1147. https://doi.org/10.1590/S0100-204X2016000900013.

Altieri, M.A., 1999. The ecological role of biodiversity in agroecosystems. Agriculture, Ecosystems and Environment 74, 19–31. https://doi.org/10.1016/S0167-8809(99)00028-6.

Alvarez, M.F., Osterrieth, M., Cooper, M., 2018. Changes in the porosity induced by tillage in typical Argiudolls of southeastern Buenos Aires Province, Argentina, and its relationship with the living space of the mesofauna: a preliminary study. Environ. Earth Sci. 77 https://doi.org/10.1007/s12665-018-7313-x.

Anghinoni, I., Vezzani, F.M., 2021. Systemic Soil Fertility as product of system self-organization resulting from management. Rev. Bras. Ciênc. Solo 45, 1–18. https://doi.org/10.36783/18069657rbcs20210090.

Atkinson, D., 2000. Root characteristics: Why and What to Measure. In: Smit, A.L., Bengough, A.G., Engels, C., van Noordwijk, M., Pellerin, S., van de Geijn, S.C. (Eds.), Root Methods: A HAndbook. Springer, Berlin Heidelberg, p. 587.

Ball, B.C., O'sullivan, M.F., Hunter, R., 1988. Gas diffusion, fluid flow and derived pore continuity indices in relation to vehicle traffic and tillage. J. Soil Sci. 39, 327–339. https://doi.org/10.1111/j.1365-2389.1988.tb01219.x.

Ball, B.C., Schjønning, P., 2002. Air permeability. In: Dane, J.H., Topp, G. (Eds.), Methods of Soil Analysis: Physical Methods. American Society of Agronomy, Madison, pp. 1141–1158.

Barral, M.P., Rey Benayas, J.M., Meli, P., Maceira, N.O., 2015. Quantifying the impacts of ecological restoration on biodiversity and ecosystem services in agroecosystems: A global meta-analysis. Agr Ecosyst Environ 202, 223–231. https://doi.org/10.1016/j.agee.2015.01.009.

Barros, E., Curmib, P., Hallaireb, V., Chauvelc, A., Lavellec, P., 2000. Role of macrofauna in the transformation and reversibility of soil structure of an Oxisol during forest to pasture conversion. Geoderma 100, 193–213.

Bayer, C., Mielniczuk, J., Amado, T.J.C., Martin-Neto, L., Fernandes, S.V., 2000. Organic matter storage in a sandy clay loam acrisol affected by tillage and cropping systems in southern Brazil. Soil Tillage Res. 54, 101–109. https://doi.org/10.1016/S0167-1987(00)00090-8.

Bayer, C., Lovato, T., Dieckow, J., Zanatta, J.A., Mielniczuk, J., 2006. A method for estimating coefficients of soil organic matter dynamics based on long-term experiments. Soil Tillage Res. 91, 217–226. https://doi.org/10.1016/j.still.2005.12.006.

Bertollo, A.M., de Moraes, M.T., Franchini, J.C., Soltangheisi, A., Balbinot Junior, A.A., Levien, R., Debiasi, H., 2021. Precrops alleviate soil physical limitations for soybean root growth in an Oxisol from southern Brazil. Soil Tillage Res. 206, 104820 https://doi.org/10.1016/j.still.2020.104820.

Betioli Junior, E., Tormena, C.A., Moreira, W.H., Ball, B.C., Figueiredo, G.C., da Silva, Á. P., Giarola, N.F.B., 2014. Aeration condition of a clayey oxisol under long-term no-tillage. Rev. Bras. Ciênc. Solo 38, 990–999. https://doi.org/10.1590/s0100-06832014000300031.

Blackwell, P.S., Green, T.W., Mason, W.K., 1990. Responses of Biopore Channels from Roots to Compression by Vertical Stresses. Soil Science Society of America Journal 54, 1088–1091. https://doi.org/10.2136sssaj1990.03615995005400040027x.

Blouin, M., Hodson, M.E., Delgado, E.A., Baker, G., Brussaard, L., Butt, K.R., Dai, J., Dendooven, L., Peres, G., Tondoh, J.E., Cluzeau, D., Brun, J.-J., 2013. A review of earthworm impact on soil function and ecosystem services. Eur. J. Soil Sci. 64, 161–182. https://doi.org/10.1111/ejss.12025.

Böhm, W., 1979. Methods of studying root systems. Springer−Verlag, Berlin Heidelberg.

Brandão, T., Trevisan, R., Both, R., 2007. Unidades de Conservação e os campos do Rio Grande do Sul. Revista Brasileira de Biociências 5, 843–845.

Brimhall, G.H., Chadwick, O.A., Lewis, C.J., Compston, W., Williams, I.S., Danti, K.J., Dietrich, W.E., Power, M.E., Hendricks, D., Bratt, J., 1991. Deformational mass transport and invasive processes in soil evolution. Science 255, 695–702.

Brundrett, M.C., 2002. Coevolution of roots and mycorrhizas of land plants. New Phytol. 154, 275–304.

Burgos Hernández, T.D., Slater, B.K., Tirado Corbalá, R., Shaffer, J.M., 2019. Assessment of long-term tillage practices on physical properties of two Ohio soils. Soil Tillage Res. 186, 270–279. https://doi.org/10.1016/j.still.2018.11.004.

Calonego, J.C., Rosolem, C.A., 2010. Soybean root growth and yield in rotation with cover crops under chiseling and no-till. Eur. J. Agron. 33, 242–249. https://doi.org/10.1016/j.eja.2010.06.002.

Campbell, G.S., 2010. Determining the 15 Bar (Permanent Wilt) water content of soils whit the WP4. Decagon Devices, Washington, DC.

Carof, M., De Tourdonnet, S., Coquet, Y., Hallaire, V., Roger-Estrade, J., 2007. Hydraulic conductivity and porosity under conventional and no-tillage and the effect of three species of cover crop in northern France. Soil Use Manag. 23, 230–237. https://doi.org/10.1111/j.1475-2743.2007.00085.x.

Chen, X., Chen, H.Y.H., Chen, C., Ma, Z., Searle, E.B., Yu, Z., Huang, Z., 2020. Effects of plant diversity on soil carbon in diverse ecosystems: a global meta-analysis. Biol. Rev. 95, 167–183. https://doi.org/10.1111/brv.12554.

Cooper, M., de Castro, S.S., Coelho, M.R., 2018. Micromorfologia do solo. In: Teixeira, P. C., Donagemma, G.K., Fontana, A., Teixeira, W.G. (Eds.), Manual De Métodos De Análise De Solos. EMBRAPA, Brasília, DF, pp. 526–564.

Cotrufo, M.F., Wallenstein, M.D., Boot, C.M., Denef, K., Paul, E., 2013. The Microbial Efficiency-Matrix Stabilization (MEMS) framework integrates plant litter decomposition with soil organic matter stabilization: Do labile plant inputs form stable soil organic matter? Glob. Chang. Biol. 19, 988–995. https://doi.org/10.1111/gcb.12113.

Cui, Z., Wu, G.L., Huang, Z., Liu, Y., 2019. Fine roots determine soil infiltration potential than soil water content in semi-arid grassland soils. J. Hydrol. 578, 124023 https://doi.org/10.1016/j.jhydrol.2019.124023.

da Silva, T.S., Pulido-Moncada, M., Schmidt, M.R., Katuwal, S., Schlüter, S., Köhne, J.M., Mazurana, M., Juhl Munkholm, L., Levien, R., 2021. Soil pore characteristics and gas transport properties of a no-tillage system in a subtropical climate. Geoderma 401. https://doi.org/10.1016/j.geoderma.2021.115222.

Da-Silva, V.L., Dieckow, J., Mellek, J.E., Molin, R., Favaretto, N., Pauletti, V., Vezzani, F. M., 2012. Melhoria da Estrutura de um Latossolo por Sistemas de Culturas em Plantio Direto nos Campos Gerais do Paraná. Revista Brasileira de Ciencia do Solo 36, 983–992. https://doi.org/10.1590/S0100-06832012000300028.

de Castro, S.S., 2008. Micromorfologia de solos: bases para descrição de lâminas delgadas, 2nd ed. Campinas Goiania.

de Moraes, M.T., Bengough, A.G., Debiasi, H., Franchini, J.C., Levien, R., Schnepf, A., Leitner, D., 2018. Mechanistic framework to link root growth models with weather and soil physical properties, including example applications to soybean growth in Brazil. Plant and Soil 428, 67–92. https://doi.org/10.1007/s11104-018-3656-z.

Dörner, J., Horn, R., 2006. Anisotropy of pore functions in structured Stagnic Luvisols in the Weichselien moraine region in N Germany. J. Plant Nutr. Soil Sci. 169, 213–220.

Durner, W., 1994. Hydraulic conductivity estimation for soils with heterogeneous pore structure. Water Resour. Res. 30, 211–223. https://doi.org/10.1029/93WR02676.

Ellies Sch, A., Grez, R., Ramírez, C., 1997. La conductividad hidráulica en fase saturada como herramienta para el diagnóstico de la estructura del suelo. Agro Sur 25, 51–56. https://doi.org/10.4206/agrosur.1997.v25n1-06.

FAO, 2020. Conservation Agriculture Principles. Rome, Italy.

Farahani, E., Emami, H., Forouhar, M., 2022. Effects of tillage systems on soil organic carbon and some soil physical properties. Land Degradation and Development 33, 1307–1320. https://doi.org/10.1002/ldr.4221.

Fischer, C., Roscher, C., Jensen, B., Eisenhauer, N., Baade, J., Attinger, S., Scheu, S., Weisser, W.W., Schumacher, J., Hildebrandt, A., 2014. How do earthworms, soil texture and plant composition affect infiltration along an experimental plant diversity gradient in grassland? PLoS One 9. https://doi.org/10.1371/journal.pone.0098987.

Fischer, C., Tischer, J., Roscher, C., Eisenhauer, N., Ravenek, J., Gleixner, G., Attinger, S., Jensen, B., de Kroon, H., Mommer, L., Scheu, S., Hildebrandt, A., 2015. Plant species diversity affects infiltration capacity in an experimental grassland through changes in soil properties. Plant and Soil 397, 1–16. https://doi.org/10.1007/s11104-014-2373-5.

Gamboa, C.H., Vezzani, F.M., Kaschuk, G., Favaretto, N., Cobos, J.Y.G., da Costa, G.A., 2020. Soil-Root Dynamics in Maize-Beans-Eggplant Intercropping System under Organic Management in a Subtropical Region. J. Soil Sci. Plant Nutr. https://doi.org/10.1007/s42729-020-00227-9.

Goebes, P., Schmidt, K., Seitz, S., Both, S., Bruelheide, H., Erfmeier, A., Scholten, T., Kühn, P., 2019. The strength of soil-plant interactions under forest is related to a Critical Soil Depth. Sci. Rep. 9, 1–12. https://doi.org/10.1038/s41598-019-45156-5.

Groenevelt, P.H., Kay, B.D., Grant, C.D., 1984. Physical assessment of soil with respect to rooting potential. Geoderma 34, 101–114.

Holthusen, D., Brandt, A.A., Reichert, J.M., Horn, R., 2018. Soil porosity, permeability and static and dynamic strength parameters under native forest/grassland compared to no-tillage cropping. Soil Tillage Res. 177, 113–124. https://doi.org/10.1016/j.still.2017.12.003.

Jones, D.L., Nguyen, C., Finlay, R.D., 2009. Carbon flow in the rhizosphere: Carbon trading at the soil-root interface. Plant and Soil 321, 5–33. https://doi.org/10.1007/s11104-009-9925-0.

Keyes, S.D., Gillard, F., Soper, N., Mavrogordato, M.N., Sinclair, I., Roose, T., 2016. Mapping soil deformation around plant roots using in vivo 4D X-ray Computed Tomography and Digital Volume Correlation. J. Biomech. 49, 1802–1811. https://doi.org/10.1016/j.jbiomech.2016.04.023.

Kravchenko, A.N., Wang, A.N.W., Smucker, A.J.M., Rivers, M.L., 2011. Long-term Differences in Tillage and Land Use Affect Intra-aggregate Pore Heterogeneity. Soil Sci. Soc. Am. J. 75, 1658–1666. https://doi.org/10.2136/sssaj2011.0096.

Labrière, N., Laumonier, Y., Locatelli, B., Vieilledent, G., Comptour, M., 2015. Ecosystem services and biodiversity in a rapidly transforming landscape in northern Borneo. PLoS One 10, 1–19. https://doi.org/10.1371/journal.pone.0140423.

Langmaack, M., Schrader, S., Rapp-Bernhardt, U., Kotzke, K., 1999. Quantitative analysis of earthworm burrow systems with respect to biological soil-structure regeneration after soil compaction. Biol. Fertil. Soils 28, 219–229. https://doi.org/10.1007/s003740050486.

Lavelle, P., Decaëns, T., Aubert, M., Barot, S., Blouin, M., Bureau, F., Margerie, P., Mora, P., Rossi, J.-P., 2006. Soil invertebrates and ecosystem services. Eur. J. Soil Biol. 42, 3–15. https://doi.org/10.1016/j.ejsobi.2006.10.002.

Lawal, H.M., Lawal, A., 2017. Pore Size Distribution and Soil Hydro Physical. Tropical and Subtropical agroecosystems 20, 111–129.

Libardi, P.L., 2016. Água no solo, in: van Lier, Q. de J. (Ed.), Física Do Solo. Sociedad Brasileira de Ciência do solo, Viçosa, MG, pp. 103–152.

Minasny, B., Stockmann, U., Hartemink, A.E., McBratney, A.B., 2016. Measuring and Modelling Soil Depth Functions. In: Hartemink, A.E., Minasny, B. (Eds.), Digital Soil Morphometrics, Progress in Soil Science. Springer International Publishing, Switzerland, pp. 425–433. https://doi.org/10.1007/978-3-319-28295-4.

Mudgal, A., Anderson, S.H., Baffaut, C., Kitchen, N.R., Sadler, E.J., 2010. Effects of long-term soil and crop management on soil hydraulic properties for claypan soils. J. Soil Water Conserv. 65, 393–403. https://doi.org/10.2489/jswc.65.6.393.

Nicoloso, D.S.R., Amado, T.J.C., Schneider, S., Lanzanova, M.E., Girardello, V.C., Bragagnolo, J., 2008. Eficiência da escarificação mecânica e biológica na melhoria dos atributos físicos de um latossolo muito argiloso e no incremento do rendimento de soja. Revista Brasileira de Ciencia do Solo 32, 1723–1734. https://doi.org/10.1590/s0100-06832008000400037.

Norris, G., Qureshi, F., Howitt, D., Cramer, D., 2014. Introduction to Statistics with SPSS for Social Science. Routledge. https://doi.org/10.4324/9781315833422.

Oberč, B.P., Arroyo Schnell, A., 2020. Approaches to sustainable agriculture: exploring the pathways towards the future of farming. Belgium, Brussels https://doi.org/10.2305/iucn.ch.2020.07.en.

Obi, M.E., 1999. The physical and chemical responses of a degraded sandy clay loam soil to cover crops in southern Nigeria. Plant and Soil 211, 165–172. https://doi.org/10.1023/A:1004609104524.

Omuto, C.T., 2009. Biexponential model for water retention characteristics. Geoderma 149, 235–242. https://doi.org/10.1016/j.geoderma.2008.12.001.

Pagliai, M., Vignozzi, N., 2002. The soil pore system as an indicator of soil quality. Advances in GeoEcology 35, 69–80.

Pawlik, Ł., Phillips, J.D., Pavel, Š., 2016. Roots, rock, and regolith : Biomechanical and biochemical weathering by trees and its impact on hillslopes — A critical literature review. Earth Sci. Rev. 159, 142–159. https://doi.org/10.1016/j.earscirev.2016.06.002.

Pedó, F., 1986. Rendimento e distribuição de raízes de seis espécies de plantas em dois níveis de compactação do solo. Universidade Federal do Rio Grande do Sul.

Pierret, A., Doussan, C., Capowiez, Y., Bastardie, F., Pagès, L., 2007. Root Functional Architecture: A Framework for Modeling the Interplay between Roots and Soil. Vadose Zone J. 6, 269. https://doi.org/10.2136/vzj2006.0067.

Pires, L.F., Borges, J.A.R., Rosa, J.A., Cooper, M., Heck, R.J., Passoni, S., Roque, W.L., 2017. Soil structure changes induced by tillage systems. Soil Tillage Res. 165, 66–79. https://doi.org/10.1016/j.still.2016.07.010.

Poulsen, T.G., 2013. Gas permeability in soil as related to soil structure and pore system characteristics. In: Logsdon, S., Berli, M., Horn, R. (Eds.), Quantifying and Modeling Soil Structure Dynamics. Soil Science society of América, Madison WI, pp. 155–185.

Prevedello, C.L., Armindo, R.A., 2015. Física do Solo com Problemas Resolvidos, 2nd ed. Curitiba Paraná Brasil.

Rabot, E., Wiesmeier, M., Schlüter, S., Vogel, H.-J., 2018. Soil structure as an indicator of soil functions: A review. Geoderma 314, 122–137. https://doi.org/10.1016/j.geoderma.2017.11.009.

Reeve, R.C., 1953. A Method for Determining the Stability of Soil Structure Based Upon Air and Water Permeability Measurements. Soil Sci. Soc. Am. J. 17, 324. https://doi.org/10.2136/sssaj1953.03615995001700040006x.

Reichert, J.M., Suzuki, L.E.A.S., Reinert, D.J., Horn, R., Håkansson, I., 2009. Reference bulk density and critical degree-of-compactness for no-till crop production in subtropical highly weathered soils. Soil Tillage Res. 102, 242–254. https://doi.org/10.1016/j.still.2008.07.002.

Reynolds, W.D., Elrick, D.E., 2002. Fallin head soil core (Tank) method. In: Dane, J., Top, C. (Eds.), Methods of Soil Analysis, Part 4 Physical Methods. Soil Science society of América, Madison WI, pp. 809–812.

Reynolds, W.D., Drury, C.F., Tan, C.S., Fox, C.A., Yang, X.M., 2009. Use of indicators and pore volume-function characteristics to quantify soil physical quality. Geoderma 152, 252–263. https://doi.org/10.1016/j.geoderma.2009.06.009.

Schäffer, B., Mueller, T.L., Stauber, M., Müller, R., Keller, M., Schulin, R., 2008. Soil and macro-pores under uniaxial compression. II. Morphometric analysis of macro-pore stability in undisturbed and repacked soil. Geoderma 146, 175–182. https://doi.org/10.1016/j.geoderma.2008.05.020.

Seki, K., 2007. SWRC fit a nonlinear fitting program with a water retention curve for soils having unimodal and bimodal pore structure. Hydrol. Earth Syst. Sci. Discuss. 4, 407–437. https://doi.org/10.5194/hessd-4-407-2007.

Sequinatto, L., Levien, R., Trein, C., R., Mazurana, M., Muller, J.,, 2014. Qualidade de um argissolo submetido a práticas de manejo recuperadoras de sua estrutura física. Revista Brasileira de Engenharia Agrícola e Ambiental 18, 344–350.

Silva, A.P., Leao, T.P., Tormena, C.A., Goncalves, A.C.A., 2009. Determinação da permeabilidade ao ar em amostras indeformadas de solo pelo método da pressão decrescente. Rev. Bras. Ciênc. Solo 33, 1535–1545. https://doi.org/10.1590/S0100-06832009000600003.

Silva, G.J., Valadão Júnior, D.D., Bianchini, A., de Azevedo, E.C., de Maia, J.C., S.,, 2008. Variação de atributos físico-hídricos em latossolo vermelho-amarelo do Cerrado mato-grossense sob diferentes formas de uso. Rev. Bras. Ciênc. Solo 32, 2135–2143. https://doi.org/10.1590/s0100-06832008000500034.

Singh, J., Singh, N., Kumar, S., 2020. X-ray computed tomography–measured soil pore parameters as influenced by crop rotations and cover crops. Soil Sci. Soc. Am. J. 84, 1267–1279. https://doi.org/10.1002/saj2.20105.

Smucker, A.J.M., Park, E., Dorner, J., Horn, R., 2007. Soil Micropore Development and Contributions to Soluble Carbon Transport within Soluble Carbon Transport within Macroaggregates. Vandose Zone Journal. https://doi.org/10.2136/vzj2007.0031.

Teixeira, P.C., Donagemma, G.K., Fontana, A., Teixeira, W.G., 2017. Manual de métodos de análise de solos, 3rd ed. EMBRAPA, Brasilia, DF.

Tisdall, J.M., Oades, J.M., 1982. Organic matter and water-stable aggregates in soils. J. Soil Sci. 33, 141–163. https://doi.org/10.1111/j.1365-2389.1982.tb01755.x.

Veloso, M.G., Cecagno, D., Bayer, C., 2019. Legume cover crops under no-tillage favor organomineral association in microaggregates and soil C accumulation. Soil Tillage Res. 190, 139–146. https://doi.org/10.1016/j.still.2019.03.003.

Veloso, M.G., Angers, D.A., Chantigny, M.H., Bayer, C., 2020. Carbon accumulation and aggregation are mediated by fungi in a subtropical soil under conservation agriculture. Geoderma 363, 114159. https://doi.org/10.1016/j.geoderma.2019.114159.

Vezzani, F.M., Mielniczuk, J., 2011a. O solo como sistema, 1st ed. Curitiba, Paraná (Brazil).

Vezzani, F.M., Mielniczuk, J., 2011b. Agregação e estoque de carbono em argissolo. Revista Brasileira de Ciencia do Solo 35, 213–223.

Weiler, M., Naef, F., 2003. An experimental tracer study of the role of macropores in infiltration in grassland soils. Hydrol. Process. 17, 477–493. https://doi.org/10.1002/hyp.1136.

Weisser, W.W., Roscher, C., Meyer, S.T., Ebeling, A., Luo, G., Allan, E., Beßler, H., Barnard, R.L., Buchmann, N., Buscot, F., Engels, C., Fischer, C., Fischer, M., Gessler, A., Gleixner, G., Halle, S., Hildebrandt, A., Hillebrand, H., de Kroon, H., Lange, M., Leimer, S., Le Roux, X., Milcu, A., Mommer, L., Niklaus, P.A., Oelmann, Y., Proulx, R., Roy, J., Scherber, C., Scherer-Lorenzen, M., Scheu, S., Tscharntke, T., Wachendorf, M., Wagg, C., Weigelt, A., Wilcke, W., Wirth, C., Schulze, E.D., Schmid, B., Eisenhauer, N., 2017. Biodiversity effects on ecosystem functioning in a 15-year grassland experiment: Patterns, mechanisms, and open questions. Basic Appl. Ecol. 23, 1–73. https://doi.org/10.1016/j.baae.2017.06.002.

Westlake, D.F., 1963. Comparisons of Plant Productivity. Biol. Rev. 38, 385–425. https://doi.org/10.1111/j.1469-185x.1963.tb00788.x.

Whelan, B.M., Koppi, A.J., McBratney, A.B., Dougherty, W.J., 1995. An instrument for the in situ characterisation of soil structural stability based on the relative intrinsic permeabilities to air and water. Geoderma 65, 209–222. https://doi.org/10.1016/0016-7061(94)00042-9.

Zhang, Z., Peng, X., 2021. Bio-tillage: A new perspective for sustainable agriculture. Soil Tillage Res. 206, 104844 https://doi.org/10.1016/j.still.2020.104844.